INTERNATIONAL ATOMIC ENERGY AGENCY
UNITED NATIONS EDUCATIONAL, SCIENTIFIC AND CULTURAL ORGANIZATION

INTERNATIONAL CENTRE FOR THEORETICAL PHYSICS
34100 TRIESTE (ITALY) - P.O.B. 586 - MIRAMARE - STRADA COSTIERA 11 - TELEPHONE: 2240-1
CABLE: CENTRATOM - TELEX 460392 - I

SMR/388 - 26

SPRING COLLEGE IN MATERIALS SCIENCE
ON
"CERAMICS AND COMPOSITE MATERIALS"
(17 April - 26 May 1989)

CREEP AND DEFORMATION
(Overheads - II)

G.S. DAEHN
Department of Materials Science and Engineering
The Ohio State University
116 W. 19th Avenue
Columbus, Ohio 43210

These are preliminary lecture notes, intended only for distribution to participants.

Theory of "Simple" Slip Creep

J. Weertman: Trans ASM, 61, 681 (1968)

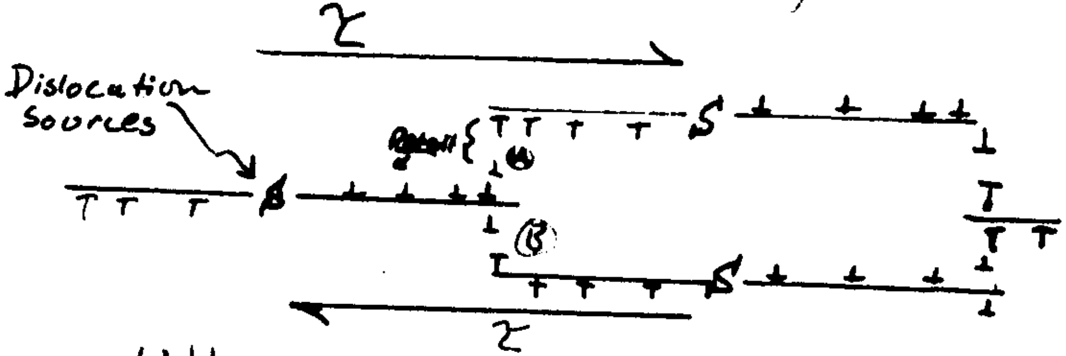

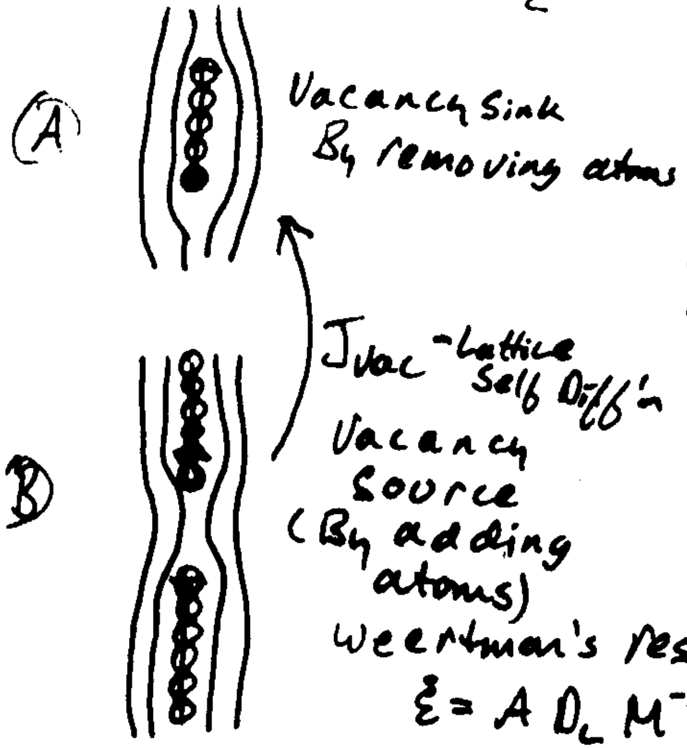

This process (movement of edge dislocation out of glide plane) is called Climb. obviously controlled by lattice self Diffusion

Weertman's result

$$\dot{\varepsilon} = A\, D_L\, M^{-\frac{1}{2}} \left(\frac{\sigma}{\mu}\right)^{3.5} \left(\frac{\sigma\,\Omega}{kT}\right)$$

M = Dislocation Source Density

Key features of the Weertman Model

$$\boxed{\dot{\varepsilon} = A\, D_L \frac{\sigma^{4.5}}{\mu^{3.5}}}$$

- Glide and climb of dislocations are sequential processes
- Vacancy flow required
- Balanced hardening and recovery.

$Q_c = Q_L$

$n = 4.5$

Despite this, the model is not truly Quantitative and is incomplete.

But it seems to capture the Essence of the Process

Now -
Consider the effect of adding a few percent Solute to a metal

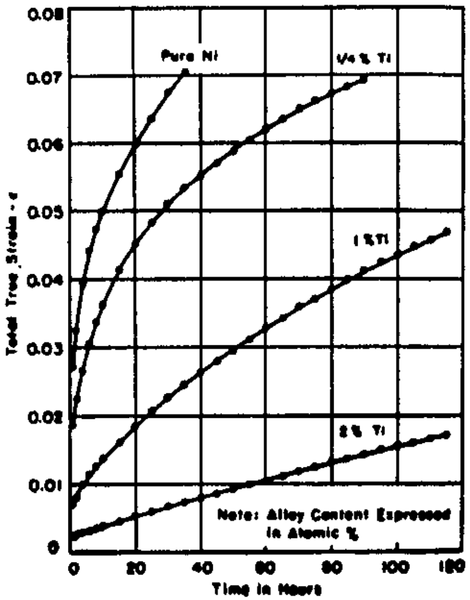

- Primary creep ~ D disappears
- the alloy becomes stronger

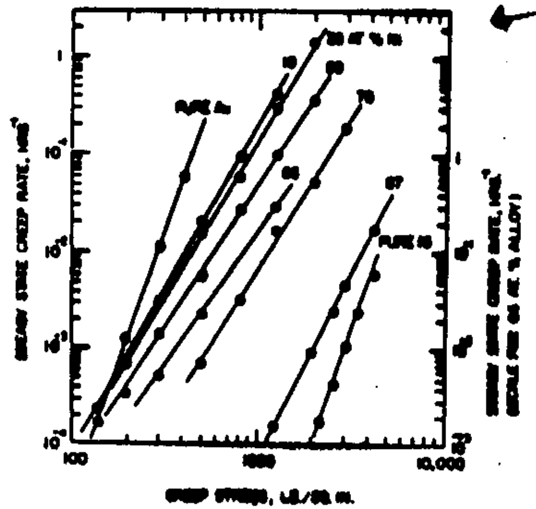

← • Alloy Stress Exponent, $n \simeq 3$ (pure Metal $\simeq 5$)

Notes on Class I creep:

① Not all alloy Systems Show Class I Behavior

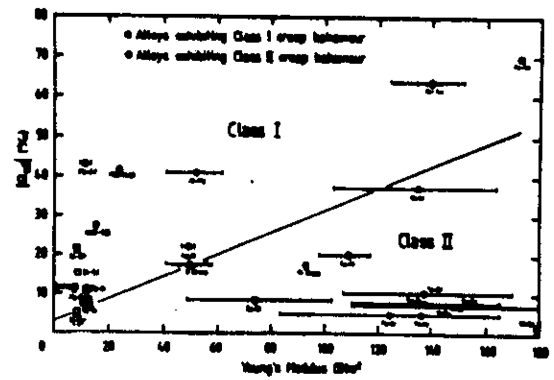

The plot shows that Systems with Large Size mismatch and Low Solvent modulus are likely to exhibit Class I Behavior.
(Class II Behavior is slip creep, discussed previously.

② Dislocation Glide and climb are Sequential processes

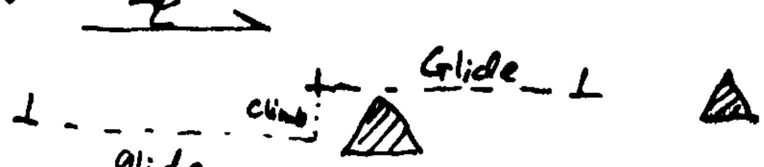

The Slower will Limit deformation

Diffusional creep is independent of these.

- Transient Behavior inverted relative to a pure metal.

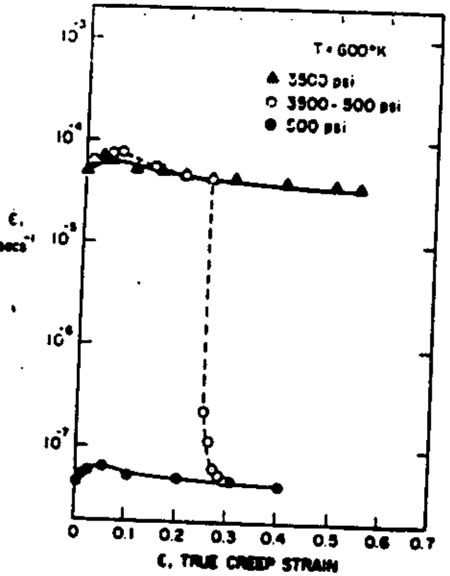

- Also Solograins Do not form, or are not important.

This is called Class I Solid Solution Creep

Theory: Impurity atoms segregate to the dislocation core, and limit the rate at which dislocations may move

$$\dot{\varepsilon} = \rho v b$$

$$\rho = C\left(\frac{\sigma}{E}\right)^2$$

$$v = \sigma D_{solute}$$ - like force...

$$\therefore \dot{\varepsilon} = C D_{solute}\left(\frac{\sigma^3}{E^4}\right)$$

Independent & Sequential Processes.

We can find a relation for each mechanism described so far.

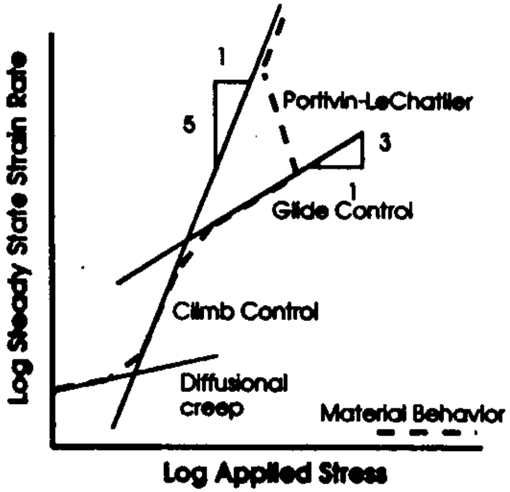

What is the overall material response

- For independent processes, add rates
- For sequential processes, the [illegible] controls.

Portevin-LeChatlier Effect
- Dislocations break away from the solute atmospheres (too fast)
- Flow is easier at higher rate

Jerky σ-ε curve results

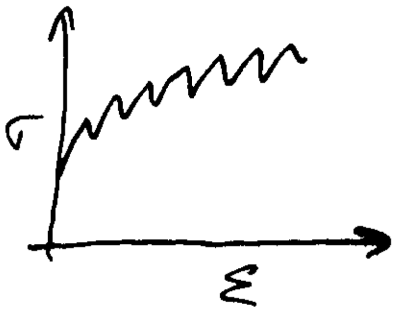

Grain boundary Sliding.

(will also be treated w/ Superplasticity)

It is well accepted that a flat, single grain boundary may slide easily at elevated temperature ($\dot{\varepsilon} \propto D_{gb}\sigma^1$)

However, other mechanisms needed due to triple points.

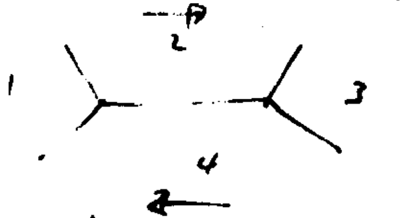

Mechanisms have been reported (well established) which give $\dot{\varepsilon} \sim 200\,\dot{\varepsilon}_{calc}$

Mechanistically still not clear.

Dispersion Hardening

Small fractions < 1% of closely spaced ~0.1 μm particles drastically change mechanical response of metal.

• Apparent threshold Stress

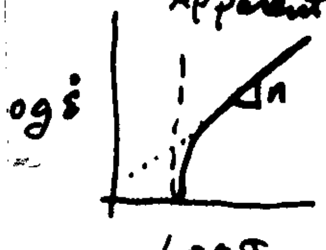

• $Q_c > Q_{SD}$ (Debated)
• Enhanced Creep Strength

Possible Explainations

• Bowing of dislocations past ppt
• dislocations "Sticking" to ppt
• Stabilization of fine "Hard" structure

Grain Boundary Sliding -and- Superplasticity

(Note: Change in Presentation order)

STRAIN RATE SENSITIVITY (m)

$$m = \frac{\partial \ln \sigma}{\partial \ln \dot{\varepsilon}}$$

m=0.5 Ideal Superplasticity

m=0.14 slip creep

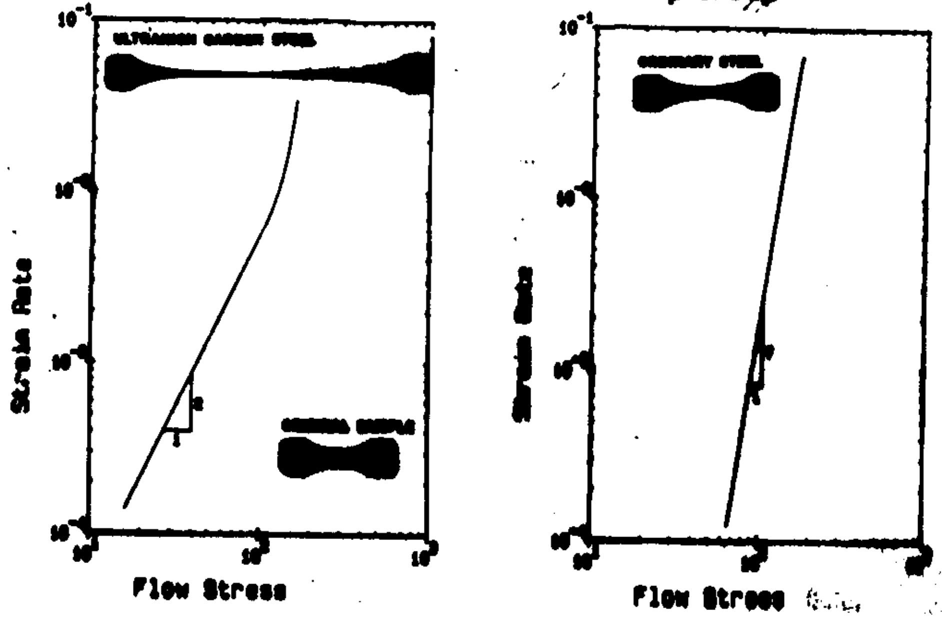

Strain rate Sensitivity and Tensile Elongation

$m = \frac{1}{n} = \frac{\partial \ln \sigma}{\partial \ln \dot{\varepsilon}}$

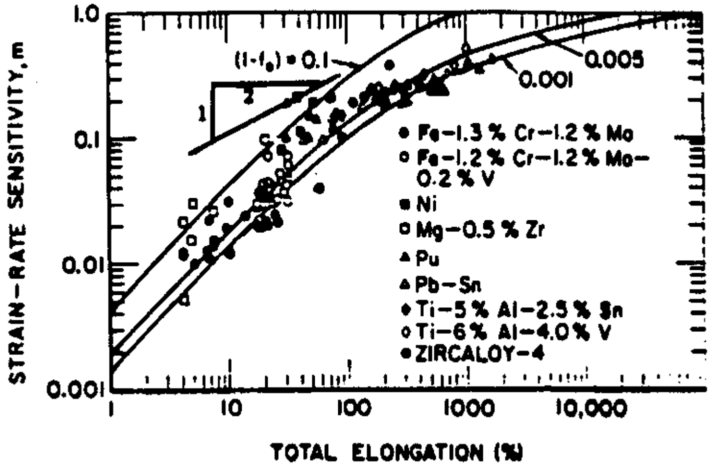

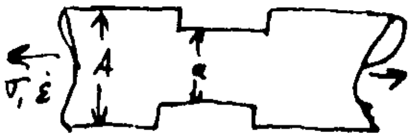

If the neck is to grow, $\dot{\varepsilon}_{neck} > \dot{\varepsilon}_{perfect}$ But if m is high...

$\sigma_{neck}^{Ao} > \sigma_{perfect}^{Ao}$ – Inhibiting neck growth

Magnitude of inequality depends on m

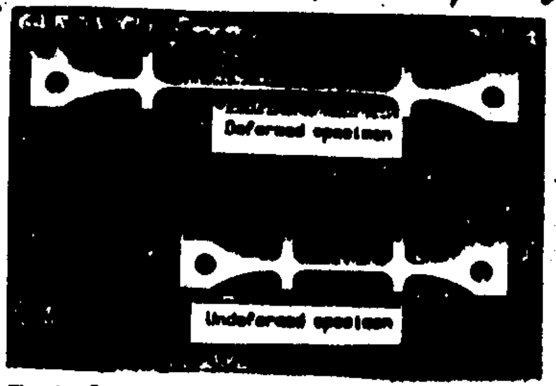

m ≈ 0…
n = 2
for ZrO…

Fig. 1. Superplastically elongated specimen of Y-TZP at 1450°C.

ZrO_2 – 3 mol% Y_2O_3 | ~0.3 μm GS

Minimum Prerequisites of Superplasticity

1) Small and stable grain size (<10μm)

   -2^d phase needed to stabilize (maybe < 1 μm for ceramics!)

2) Boundaries can support tensile stress

3) High angle grain boundaries present

Empirical View on Superplastic Deformation

Grain boundary sliding is responsible

$$\dot{\varepsilon}_{Sbs} = 2\times10^{-9} D_{eff} \left(\frac{1}{d}\right)^2 \left(\frac{\sigma}{E}\right)^2$$

(This Eq'n is found to work well for metals as well as for Wakai's recent experiments on $ZrO_2 - Al_2O_3$ Composites)

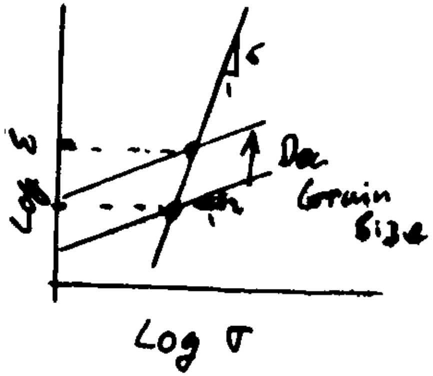

Note: There is a Maximum Strain rate Available for Superplastic Deformation (Elongation decreases as rate continues to increase

• In the Case of ZrO_2 the Key seems to have been:
  • Supression of Void Growth (Possibly by low req'd flow Stress for fairly rapid deformation)

not in increasing the rate Sensitivity of deformation.

Microstructural Changes in Superplastic Deformation

1) Grain growth

2) Discrete motion across grain boundaries

3) Grain rotation

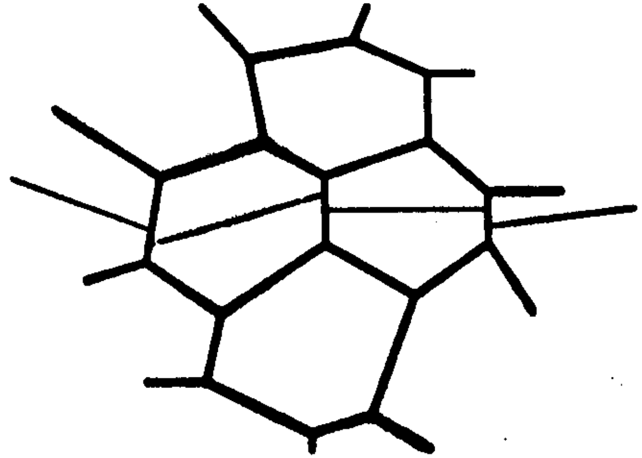

4) Grains remain equiaxed

5) Texture usually destroyed

Theoretical Approaches to S. P. D.

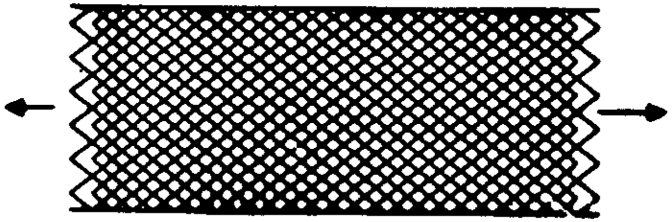

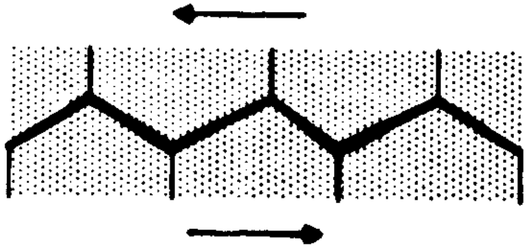

Key Problem is how can the boundary slide and accomodate the effects?

Some Proposed Mechanisms for S.P.D.:

1) Deformation by lattice diffusion
2) Deformation by grain boundary diffusion
3) GBS with diffusional accomodation
4) GBS with accomodation by slip
5) GBS accomodated by boundary migration.
6) Different Behavior in the near-boundary regi

Grain Growth in Superplastic Deformation

1) Dynamic G.G. >> Static G.G.

2) (Growth/strain) higher at low $\dot{\varepsilon}$

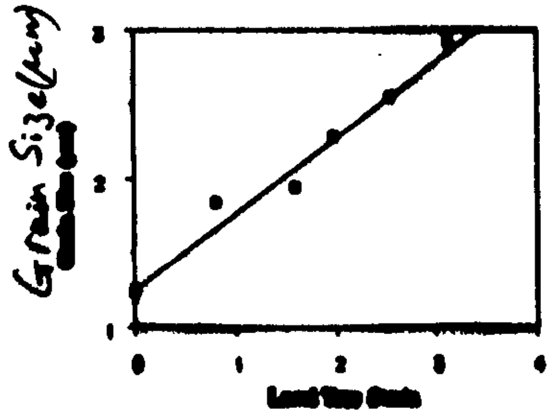

The Big Picture View - The [illegible]

Process Controlls d[illegible]

A Short Catalog of Creep Mechanisms

Mechanism	Temp. Dependence*	Stress Dependence	Structure Dependence	Conditions Where Observed
Diffusional				
Nabarro-Herring	D_l	$(\sigma/E)^1$	d^{-2}	Fine grains, low stress, hi T
Coble Creep	D_{gb}	$(\sigma/E)^1$	d^{-3}	Fine grains. low stress, hi T
Slip				
Viscous Glide (Class I Solid Sol.)	D_l	$(\sigma/E)^3$	$e^{-2} c^{-1}$	Misfitting solutes – Glide controls creep. Climb and glide are sequential
Weertman's Climb Model	D_l	$(\sigma/E)^{4.5}$	$M^{-0.5}$	Pure Metals
Lattice Diff. Cont (Phenomenological)	D_l	$(\sigma/E)^5$	Stress fixes structure	Coarse grains, T>0.6Tm
Pipe diffusion control (Phenomenological)	D_p	$(\sigma/E)^7$	"	As above T= 0.4 to 0.6 Tm
Constant Structure D_l (Phenomenological)	D_l	$(\sigma/E)^8$	χ^0	Constant Structure Tests and ODS alloys T>0.6 Tm
Constant Structure D_p (Phenomenological)	D_p	$(\sigma/E)^{10}$	χ^0	As above, lower Temp range

Grain Boundary Sliding (Phenomenological)				
Lattice Diff. Cont.	D_l	$(\sigma/E)^2$	d^{-2}	Fine grains, intermed. T and σ
Pipe Diff. Cont.	D_p	$(\sigma/E)^4$	d^{-2}	As above, but lower T.
G. B. Diff. Cont.	D_{gb}	$(\sigma/E)^2$	d^{-3}	As above, maybe finer G.S.
Others				
Harper-Dorn Creep	D_l	$(\sigma/E)^1$	-	High T, Low σ, Coarse Grains

---

Terms

Subscripts
l- Lattice Diffusion
p- Diffusion along dislocation pipes
gb- Grain Boundary Diffusion

The General Forms:

$$\dot{\varepsilon}_{ss} = A\, D_{eff}\, S \left(\frac{\sigma}{E}\right)^n$$

$$D_{eff} = D_l + B\, D_{gb} + C\, D_p$$

$$D_X = D_X^0 \exp\left(\frac{-Q_X}{RT}\right)$$

Symbols
E- Dynamic Elastic Modulus
L- Linear Intercept G. S. (or interparticle size)
d- Grain Diameter =1.76 L
λ- L. I. Subgrain size
e- Fractional size diff. between solvent & solute atoms
c- Concentration of solute atoms
S- Generalized Structure Function
n- Stress exponent (n=(1/m); m-strain rate sensitivity exp)
M- Dislocation Source Density

An Example

Assume 10μm G.S. Pure Metal at ~ 0.7 Tm

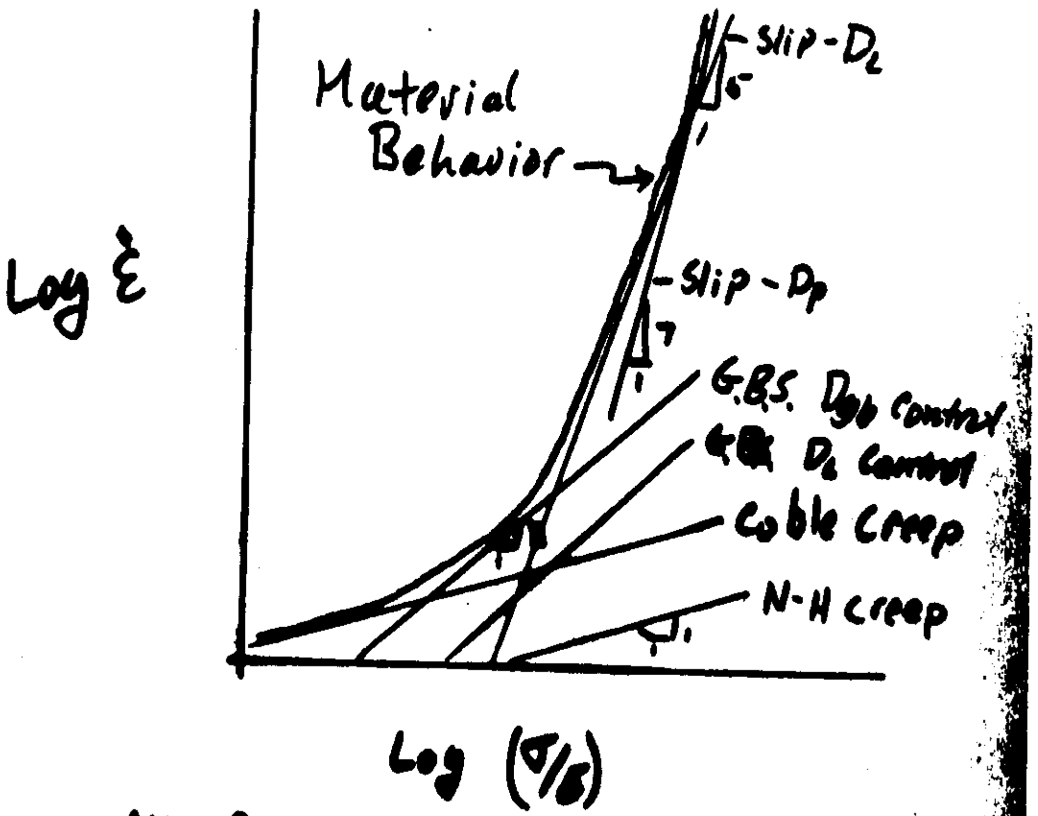

All of the above are independent Processes

Deformation Mechanism Maps

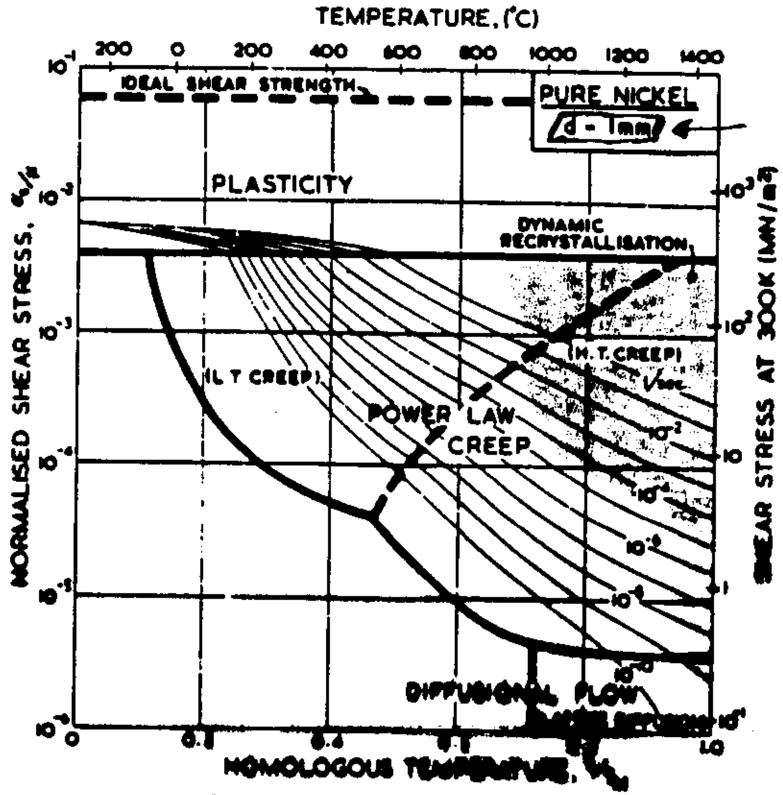

This is really complimentary with the last approach -- for independent Processes, Just compare the rates for all known Processes at a given σ/E and T. The fastest process dominates

(Similarly, Fracture Mechanism maps now exist, too!)

Comparison of Creep in Metals and Ceramics

Overall Quite Similar:

- Coble Creep
- Nabarro-Herring Creep
- Harper-Dorn Creep
- Superplasticity via Grain boundary Sliding

Have all been demonstrated in metallic and ceramic systems.

Furthermore, $n=3$ and $n=5$ has been documented in many Ceramics as well

$n \approx 5$			$n \approx 3$	
KCl	KBr	ThO_2	Al_2O_3	BeO
LiF	NaCl	WC	MgO	UC
UO_2	CaO	BeO	Si_3N_4	KCl-NaCl (Solid Solution)
Cu_2O	UN			

While there has been far less work on Ceramics in this high-stress Exponent area, it seems the same explainations can be applied.

$n=5 \rightarrow$ recovery Control, Subgrain formation, etc

$n=3 \rightarrow$ interaction w/ dislocation cores (easy to rationalize in Multi-Component Systems)

There are also important differences Between Classical Metal & ceramic creep

1) Dislocation Structure
   - Larger Burgers vector

• — ⊙ Can dissociate to a wide variety of partials
  - Often Syncronized Shuffling required in two adjacent atom planes

A — ⊙ Possible for partials to climb apart, Locking the dislocation
   - Kinks & Jogs in Ionics can be Charged

? — ⊙ Different Slip Systems are activated upon changing stress or temperature (leads, often, to ductility @ high temp)

Unusual effects can be seen b/c A, B and C above can be seen as changing Available mechanisms

Example Al_2SiO_5 – Strength increases from 500°C – 900°C.

Explaination – partial dislocations dissociate out of the glide plane, Immobilizing them.

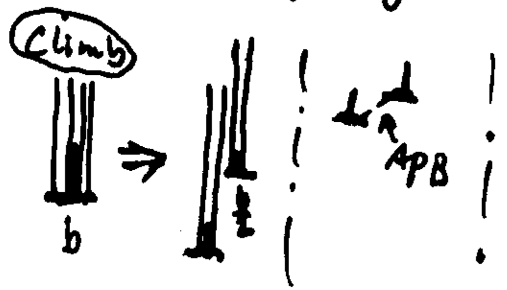

These effects also seen in ordered intermetallics

• Effect of Glassy Phases

A. Large Volume fractions of Glass

- Well known that glass deforms in a viscous ($n=1$) manner
- Free Volume Theory* Explains flow Well

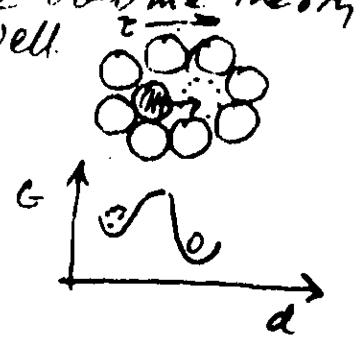

This theory can Explain viscosity changes with time (changes in V_f)

∴ for large volume fractions Glass Deformation may occur by viscous flow and crystalline grains may be carried like "logs in a river".

B. Glassy Grain Boundary films

1) They can promote Grain boundary sliding
2) Diffusion through the glass Enhances Coble-like creep†

---

* D. Turnbull & M.H. Cohen: J. Chem Phys 34, 120 (1961)
F. Spaepen: Acta Met 25, 407 (1977)
† G.M. Pharr and M.F. Ashby: Acta Met 31, 129 (19[illegible])

Creep via Dissolution & re-Precipitation

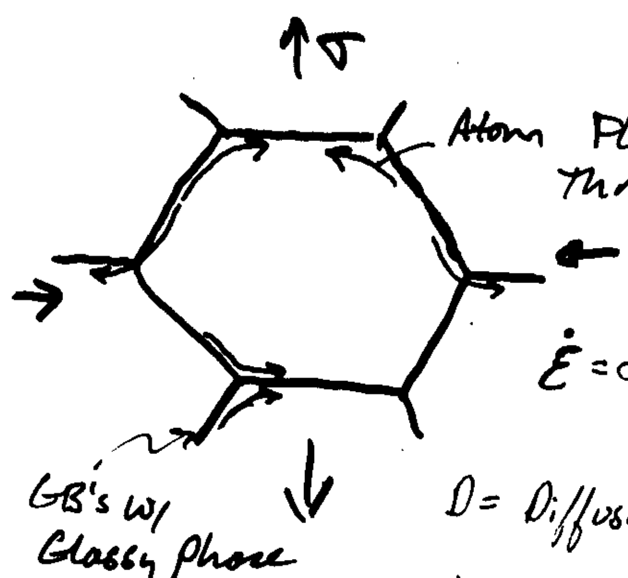

$$\dot{\varepsilon} = \alpha \frac{D c h \sigma}{k T d^3}$$

D = Diffusion coefficient of slowest species in Glass
c = Solute concentration of slowest species in the Glass
h = Glass layer thickness

Note: Devitrification will reduce creep rate

3. Diffusion in Ceramics

- Creep is diffusion controlled!

Thus, O_2 partial pressure will affect the creep rate of oxides

And impurities are very important

These effects are well documented & further support the concept of diffusion control in creep.

4. Cracks & Stress State

For Plasticity (Isotropic) Creep Properties Should be identical in Tension & Compression

- Strain can occur by cracking
  - not an isotropic process!

If a ceramic is quite prone to cracking, higher rates of flow may be seen in tension due to Void & crack Growth.

Fracture at Elevated Temperature

BROAD CLASSES OF FRACTURE MECHANISM

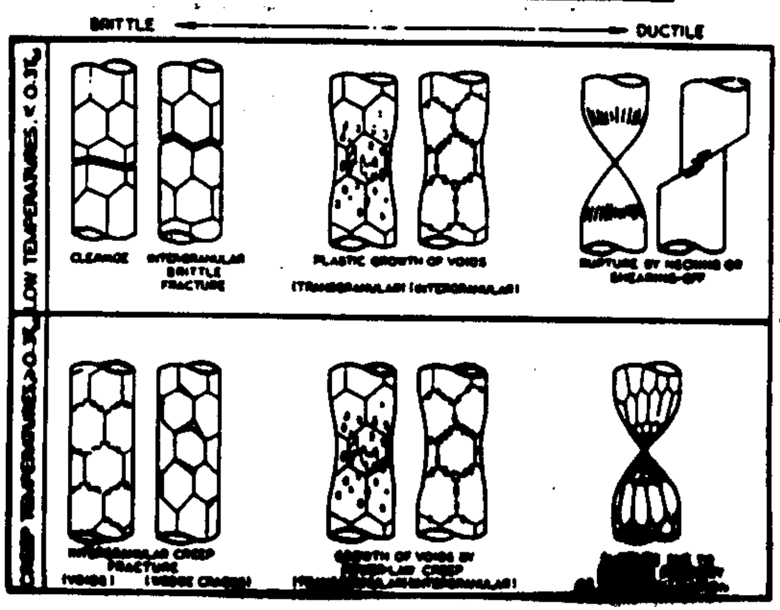

Brittle Fractur[e] especial[ly] for cera[mics]

The Growth and interlinking of voids is the usual mechanism of high Temperature fracture.

The mechanistics of this process are essentially the same as those discussed so far ...

Classical Nucleation theory cannot explain the early appearance of voids...

But these kinds of ideas can

MECHANISMS OF INTERGRANULAR CAVITY NUCLEATION

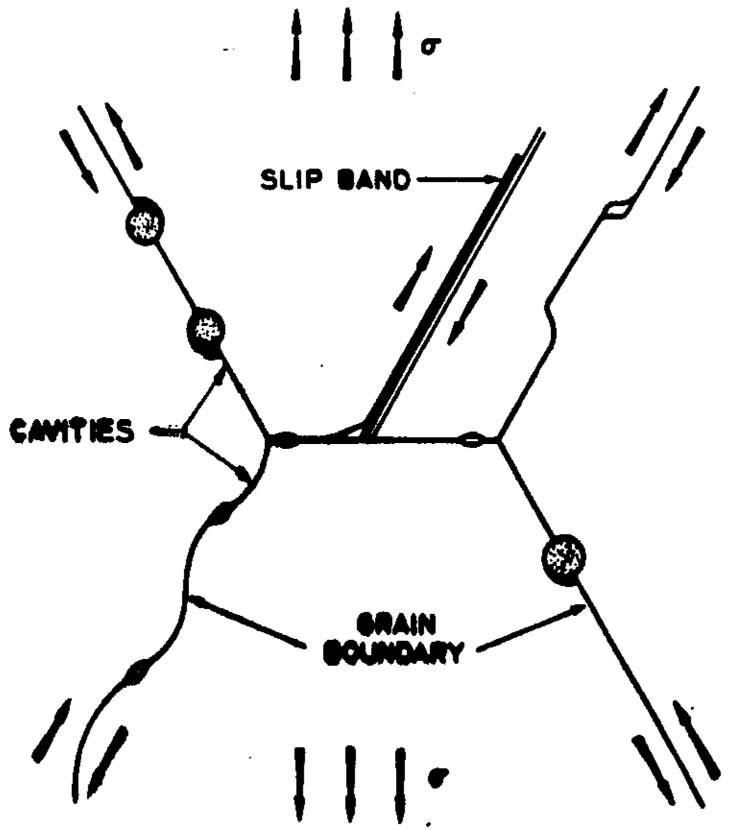

Growth of Cavities

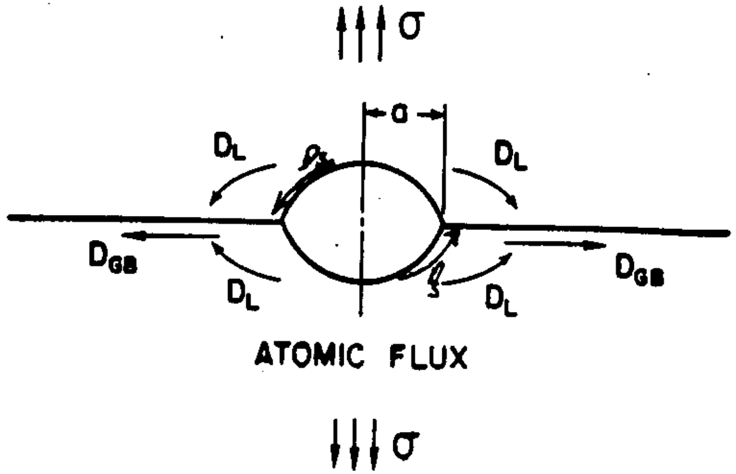

These concepts yield,

$$\frac{da}{dt} = A \, D_{gb} \, \sigma$$

Where σ is best interpreted as a local stress

For isolated cavities growth is coupled to deformation of the surrounding matrix

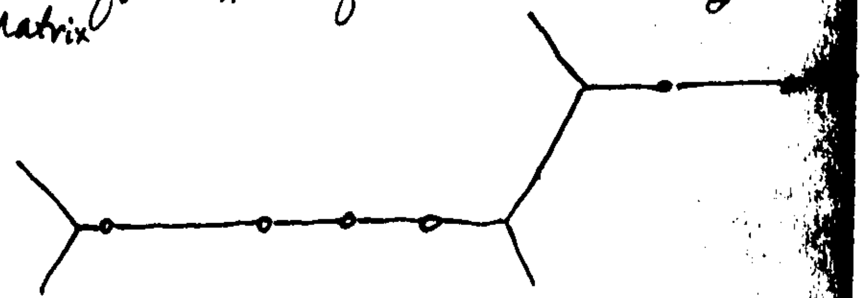

The [illegible] Deformation and Cavity growth is apparent in the Grant Monkman relation –

$$t_r = \frac{\dot{\varepsilon}_{ss}}{\dot{\varepsilon}_{GM}}$$

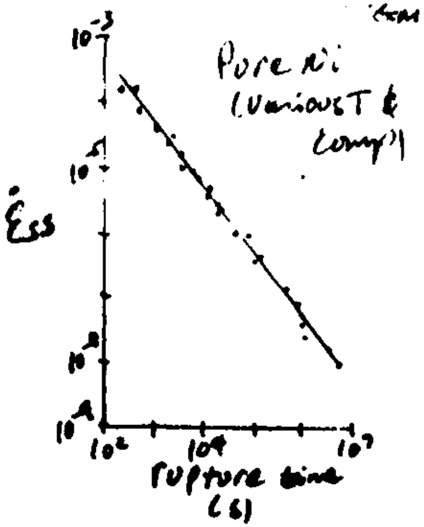

By this thinking the voiding G.B's shed load as time goes on.

Recently Anderson & Rice treated this prob and found the principal Facet Stresses on Grain boundaries for Creeping, voiding materials.

[illegible] used part of the Anderson analysis to estimate the principal Facet Stress as

$$\sigma_f = 2.24\,\sigma_1 - 0.62\,(\sigma_2 + \sigma_3)$$

This approach has been used very [illegible] to predict [illegible] under multiaxial stress (A vexing problem until recently)

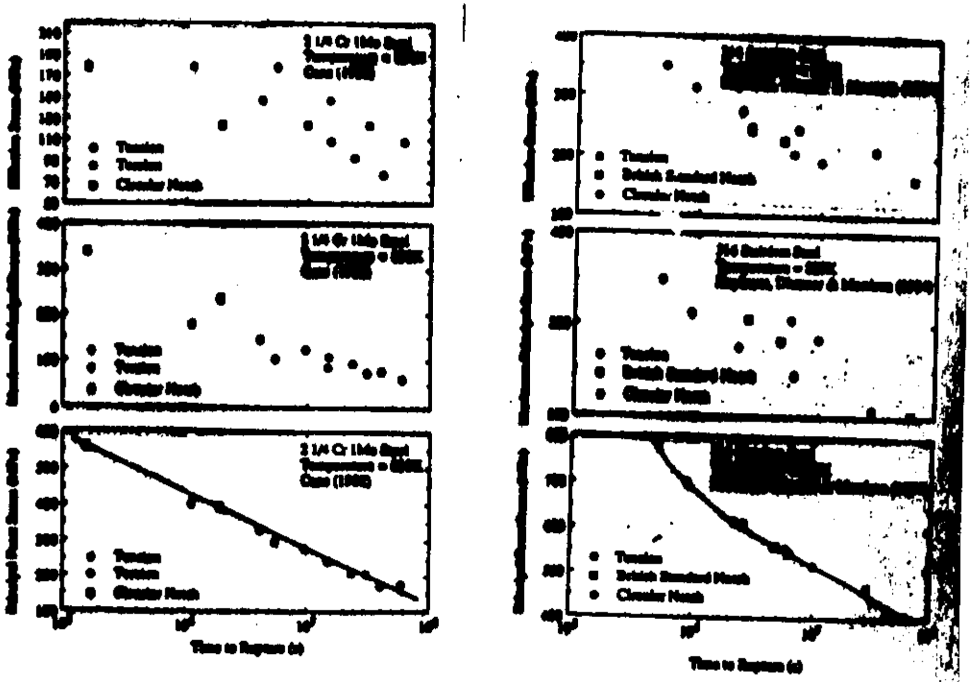

Creep of Composite Materials

Classes:

1) Continuous Reinforced Composites

β fibers in α matrix

$\sigma_{Ap} = V_\alpha \sigma_\alpha + V_\beta \sigma_\beta$

– and –

$\dot{\varepsilon}_\alpha = \dot{\varepsilon}_\beta$

(isostrain rule of mixture)

2) Discontinuous Reinforced composites

Usually the fibers are much stronger than the matrix. Matrix flows with fibers "along for the ride".

Two Separate & important effects

1) restriction of deformation, mechanical
 – like dispersion hardening
 n & Q_c may change due to changes in rate limiting step

...y to a – isotropic

2) The Geometry of deformation changes
 – higher stresses are required
 – This is a very Anisotropic Effect

"Internal Stress" or "Environmental" Superplasticity

Conditions:

- Thermal cycling of a material containing an internal thermal expansion mismatch. (α-uranium, zinc, Al-SiC, etc.)
- Thermally cycling a material through a phase transformation. (Fe $\alpha \leftrightarrow \gamma$, etc.)*

Features:

- Plastic flow well below macroscopic "yield" stress.
- Strain-rate-sensitivity-exponent of unity at low stress.
- Superplastic tensile ductility.
- No primary creep.

* In transformation plasticity $\varepsilon_{Trans} = A \left(\frac{\Delta V}{V}\right)\left(\frac{\sigma}{\sigma_{?}}\right)$

Bradt, Hoke, et al† have demonstrated this effect in Bi_2O_3, Bi_2O_3–Sm_2O_3, Bi_2WO_6 and Bi_2MoO_6.
In Bi_2WO_6 ~ 0.6 true strain on one thermal cycle

† J.A.C.S. 58, 37 (1975); 58 381 (1975); 63 292 (...

Observations of Al-SiC_w Tested under Thermal Cycling & Isothermal Conditions

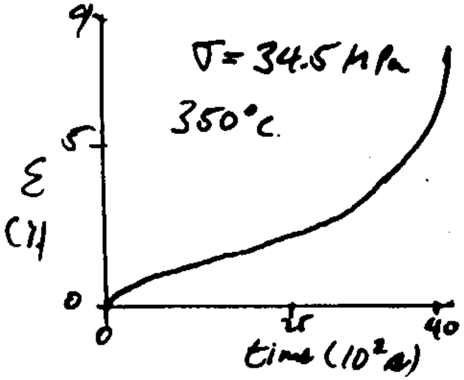

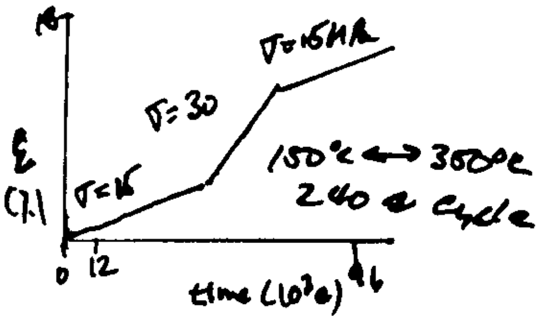

1. No primary creep under cycling
2. faster creep under cycling (even @ lower σ and Temp)
3. Higher creep ductility
4. ε̇ appears proportional to stress

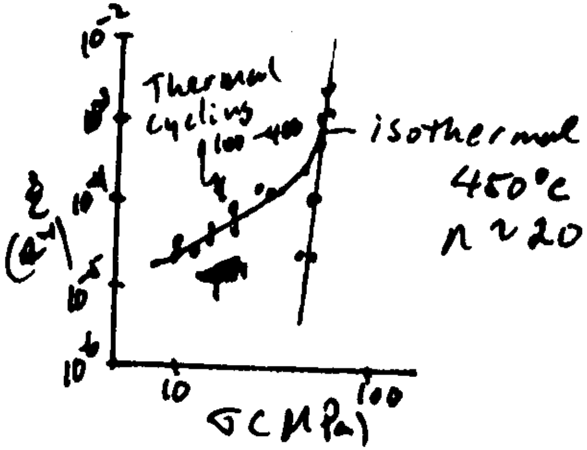

High Strain Rate Sensitivity + Slow Void Growth

= Superplasticity!

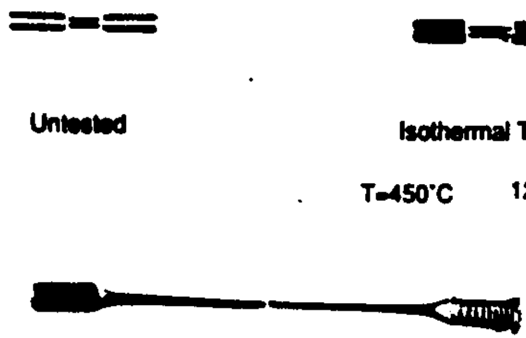

Untested

Isothermal Tension

T=450°C 12% Elongation

Thermal Cycling Tension

T= 100-450°C 1400% Elongation

Al + 20% SiC

Cycling 100°C ↔ 450°C

Application to Whisker Reinforced Composites:

The real stress state is complicated, and has tremendous spatial variation...

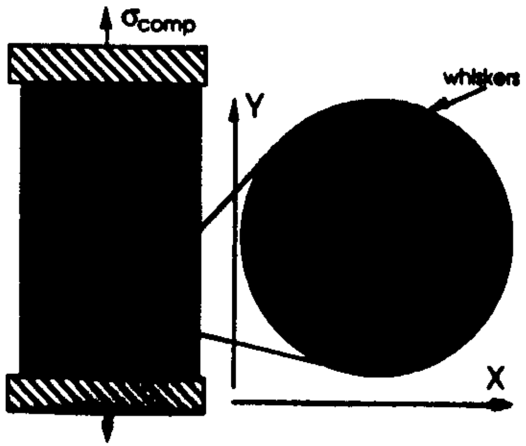

Consider this ***approximate*** geometry...
(can consider a single matrix element)

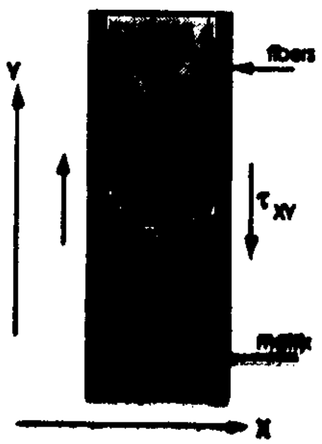

A First-Order Model

Assumptions:

- Perfect bonding at fiber/matrix interface.
- vonMises material with T independent flow stress σ_o.
- Composite externally loaded in shear.
- Temperature change induces axial stress.

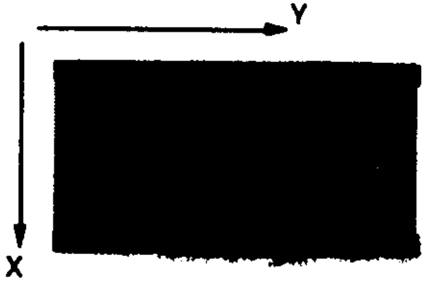

Treat with Levy-vonMises Equations:

$$d\varepsilon_{ij} = \frac{3}{2}\frac{d\bar{\varepsilon}}{\bar{\sigma}}\sigma'_{ij}$$

where σ'_{ij} is the stress state, less the hydrostatic component.

On heating:

$$\sigma_{ij} = \begin{bmatrix} 0 & \tau_{xy} & 0 \\ \tau_{xy} & \sigma_y & 0 \\ 0 & 0 & 0 \end{bmatrix}$$

On cooling:

$$\begin{bmatrix} 0 & \tau_{xy} & 0 \\ \tau_{xy} & -\sigma_y & 0 \\ 0 & 0 & 0 \end{bmatrix}$$

$$\sigma'_{ij} = \begin{bmatrix} \frac{\sigma_y}{3} & \tau_{xy} & 0 \\ \tau_{xy} & \frac{2\sigma_y}{3} & 0 \\ 0 & 0 & \frac{\sigma_y}{3} \end{bmatrix} \qquad \begin{bmatrix} \frac{-\sigma_y}{3} & \tau_{xy} & 0 \\ \tau_{xy} & \frac{-2\sigma_y}{3} & 0 \\ 0 & 0 & \frac{-\sigma_y}{3} \end{bmatrix}$$

since the Levy-vonMises Equation holds:

$$d\varepsilon_{ij} = \frac{3}{2}\frac{d\bar{\varepsilon}}{\bar{\sigma}}\sigma'_{ij}$$

After a full temperature cycle, everything but the shear cancels out!

Then we can calculate shear strain per cycle as...

$$\gamma_{xy} = 6\left(\frac{\Delta\alpha(\Delta T - \Delta T_{crit})}{\sqrt{\sigma_0^2 - 3\tau_{xy}^2}}\right)\tau_{xy}$$

Conclusion:

If temperature change induces plastic deformation, very small stresses will induce plastic strain. The magnitude of that strain will be proportional to the applied stress, the thermally induced plastic strain and inversely proportional to the matrix flow stress.

MODEL ASSUMPTIONS:

- Two-dimensional problem.
- Fibers deform elastically only.
- Matrix has elastic and plastic, power-law creep, behavior.
- All axial load is transmitted through the matrix as a shear stress.
- Composite elongates by shearing of the matrix between fibers.
- Bonding perfect at fiber / matrix interface

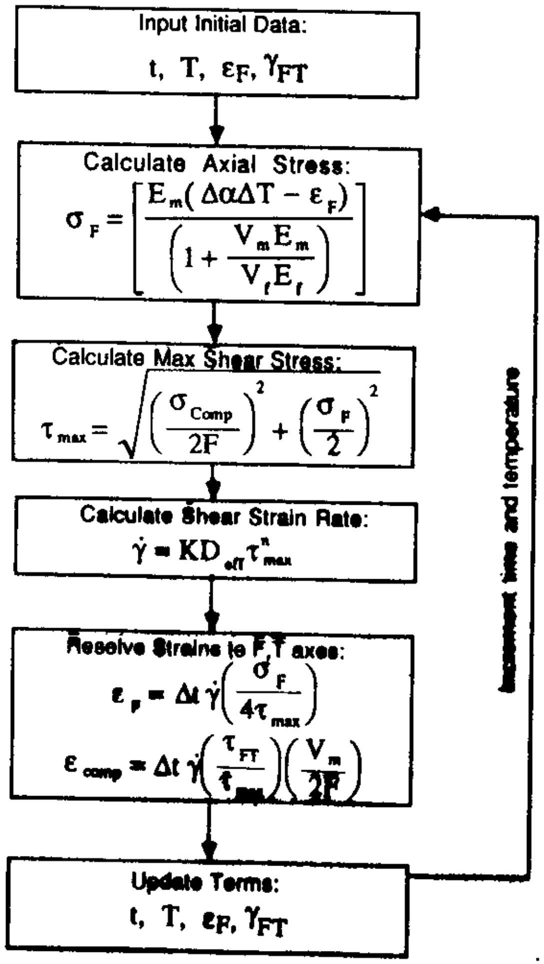
Input Initial Data:
t, T, ε_F, γ_{FT}
Calculate Axial Stress:
$\sigma_F = \left[\frac{E_m(\Delta\alpha\Delta T - \varepsilon_F)}{\left(1 + \frac{V_m E_m}{V_f E_f}\right)}\right]$
Calculate Max Shear Stress:
$\tau_{max} = \sqrt{\left(\frac{\sigma_{Comp}}{2F}\right)^2 + \left(\frac{\sigma_F}{2}\right)^2}$
Calculate Shear Strain Rate:
$\dot{\gamma} = K D_{eff} \tau_{max}^n$
Resolve Strains to F, T axes:
$\varepsilon_F = \Delta t\, \dot{\gamma}\left(\frac{\sigma_F}{4\tau_{max}}\right)$
$\varepsilon_{comp} = \Delta t\, \dot{\gamma}\left(\frac{\tau_{FT}}{\tau_{max}}\right)\left(\frac{V_m}{2F}\right)$
Update Terms:
t, T, ε_F, γ_{FT}
Increment time and temperature

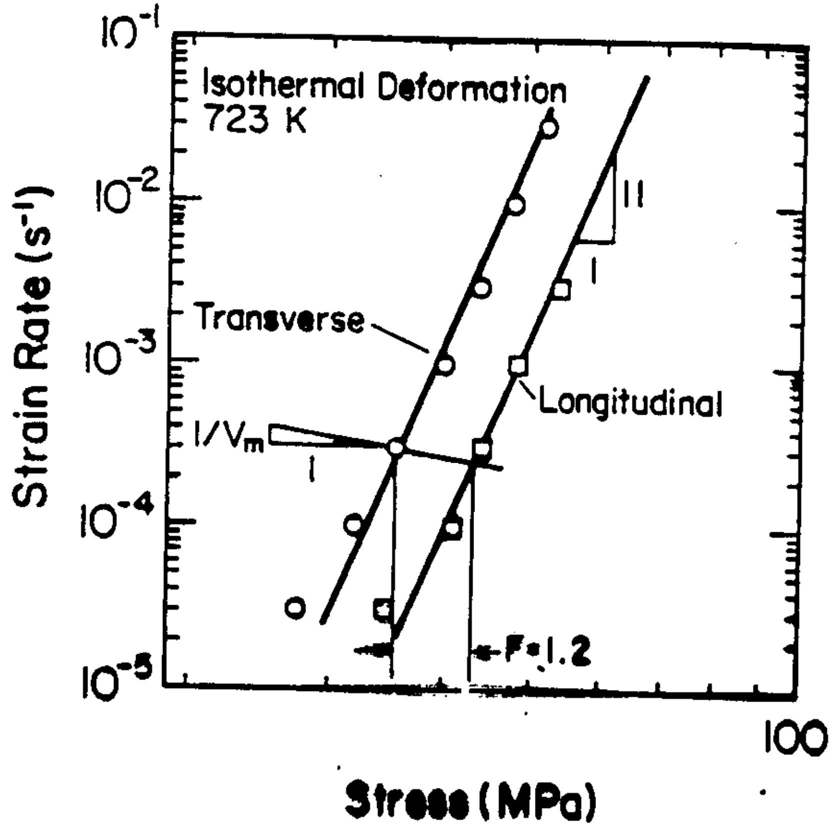
Isothermal Deformation
723 K
Transverse
Longitudinal
$1/V_m$
1
11
1
F=1.2
Strain Rate (s^{-1})
10^{-1}
10^{-2}
10^{-3}
10^{-4}
10^{-5}
100
Stress (MPa)

Constants Used in Simulation of MMC Deformation

Aluminum Diffusion Data

D_{0l} (m^2/s)	D_{0p} (m^2/s)	Q_l (KJ/mole)	Q_p (KJ/mole)
1.7×10^{-4}	2.8×10^{-6}	142	82

Composite Creep Constants & Geometric Factor

Material	n	K	F
6061-20% SiC	11	1.07×10^{-3}	1.2

Component Physical Properties

Component	E (MPa)	α (C^{-1})	Vol Fract
Al	55,000	24×10^{-6}	0.8
SiC	510,000	4.6×10^{-6}	0.2

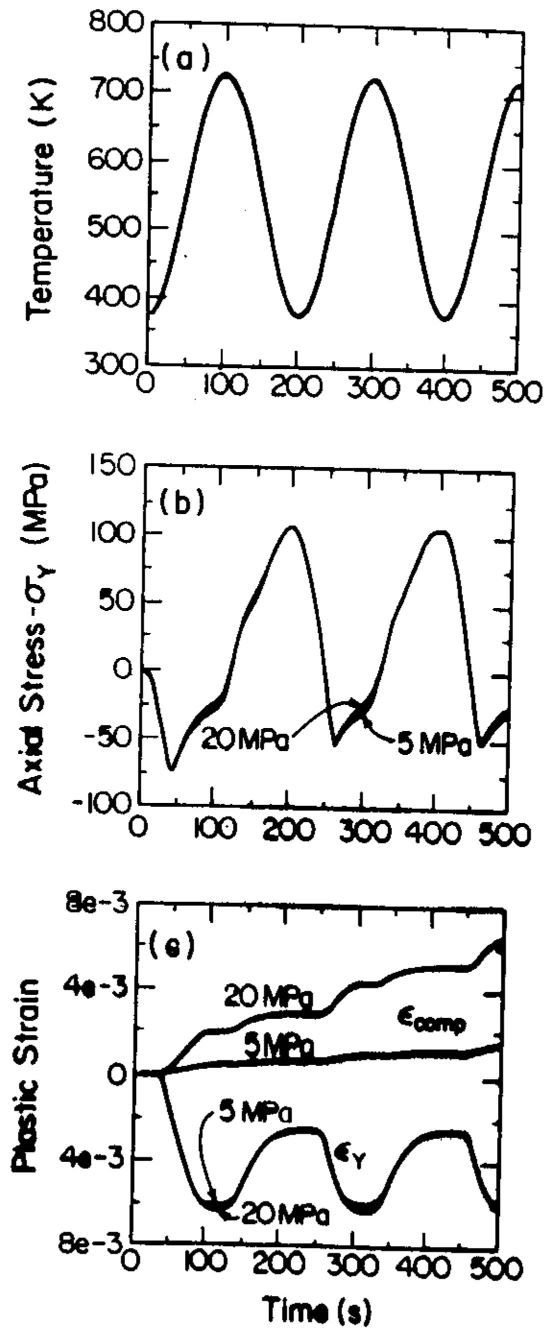

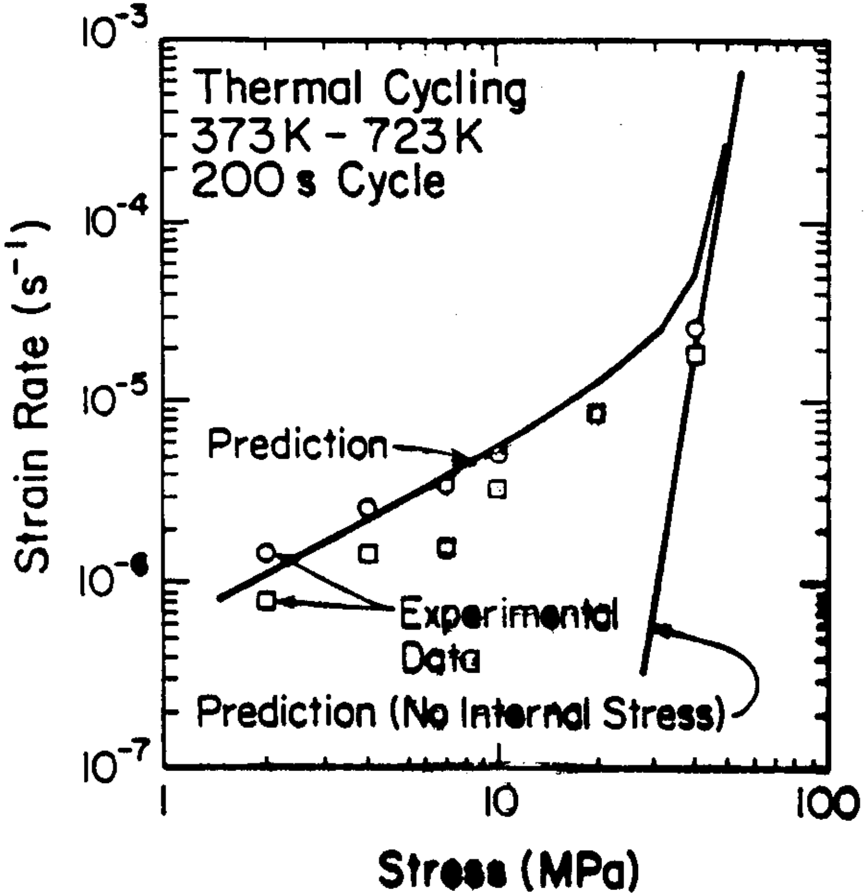

Thermal Cycling
373 K - 723 K
200 s Cycle
Prediction
Experimental Data
Prediction (No Internal Stress)
Strain Rate (s⁻¹)
Stress (MPa)

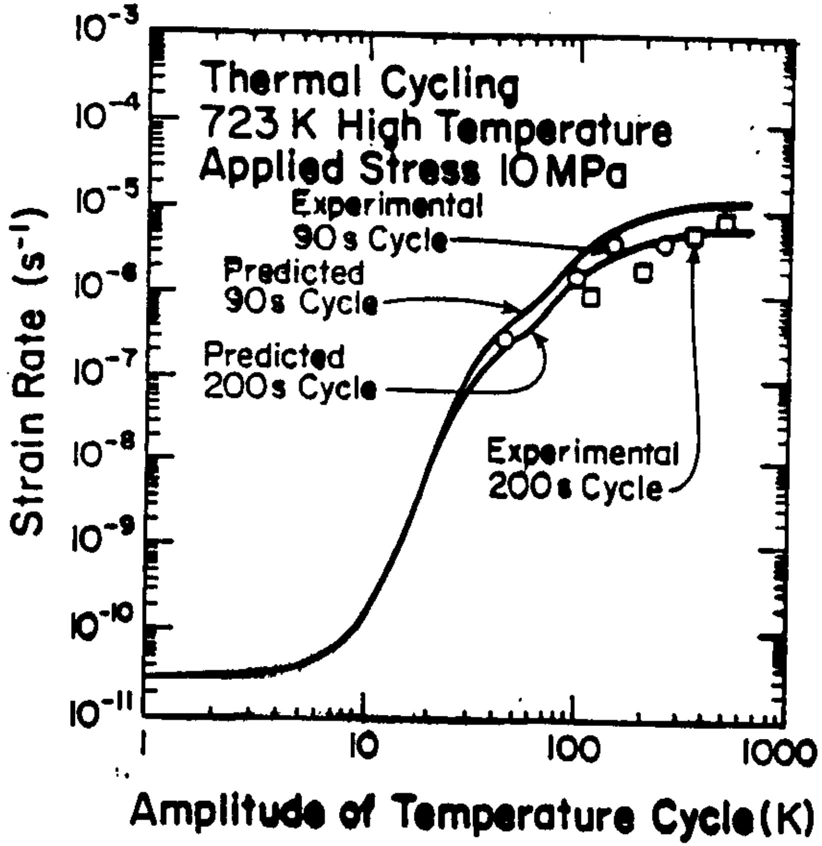

Thermal Cycling
723 K High Temperature
Applied Stress 10 MPa
Experimental 90 s Cycle
Predicted 90s Cycle
Predicted 200s Cycle
Experimental 200 s Cycle
Strain Rate (s⁻¹)
Amplitude of Temperature Cycle (K)

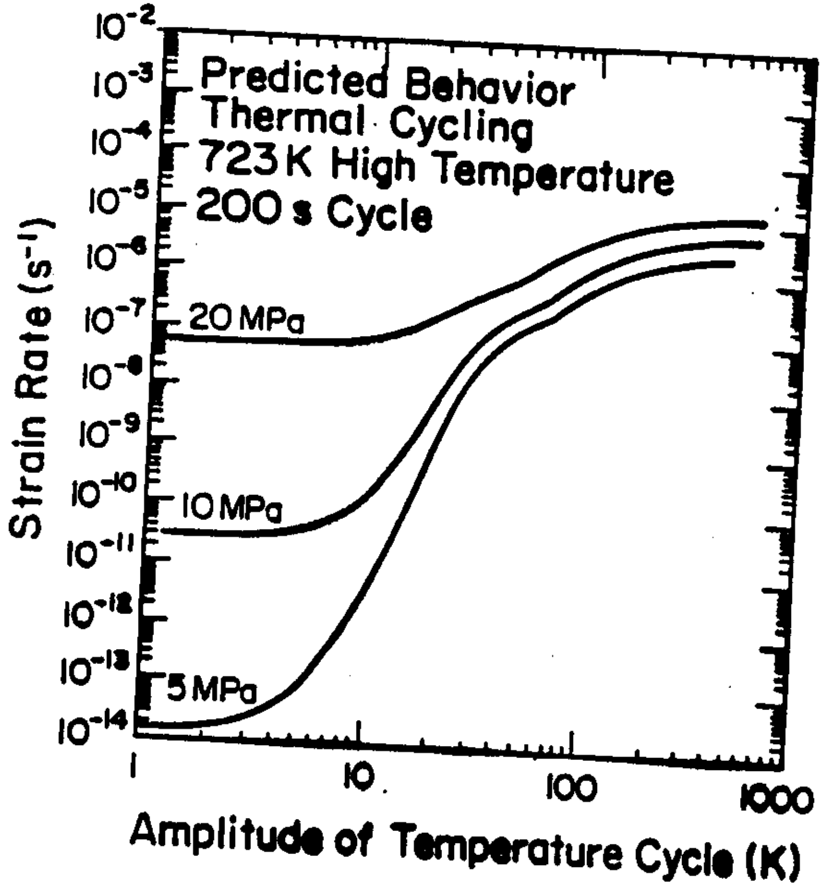
Predicted Behavior
Thermal Cycling
723 K High Temperature
200 s Cycle
20 MPa
10 MPa
5 MPa
Strain Rate (s⁻¹)
Amplitude of Temperature Cycle (K)
1
10
100
1000

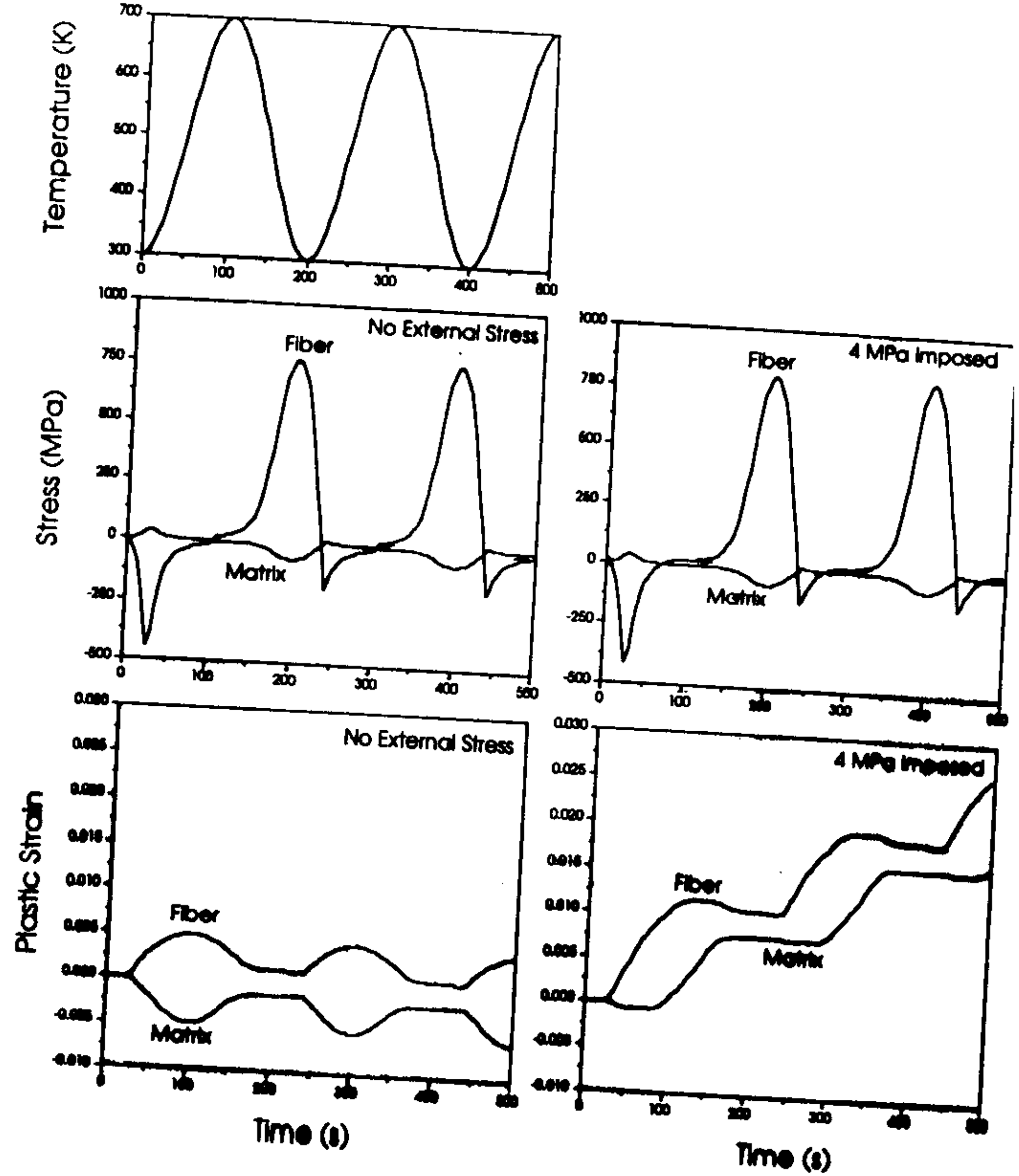
Temperature (K)
No External Stress
4 MPa imposed
Fiber
Matrix
Stress (MPa)
Plastic Strain
Time (s)

Thermal Cycling of Continuous-Fiber Reinforced Composites

Fundamental Relationships:

Load Equilibrium

$$\sigma_{ext} = V_f \sigma_f + V_m \sigma_m$$

Length Equilibrium

$$\alpha_f \Delta T + \varepsilon_f^{pl} + \left(\frac{\sigma_f}{E_f}\right) = \alpha_m \Delta T + \varepsilon_m^{pl} + \left(\frac{\sigma_m}{E_m}\right)$$

Assume Both are Elastic With Plastic Response:

$$\dot{\varepsilon} = K \exp\left(\frac{-Q_c}{RT}\right)\sigma^n$$

Pick Reasonable (but arbitrary) constants:

	Matrix	Fiber
V_f	0.9	0.1
E (MPa)	55,000	500,000
α ($C^{-1} \times 10^{-6}$)	30	5
Qc (KJ/mol)	75	150
K ($s^{-1} MPa^{-n}$)	75,000	1×10^{-6}
n	4	7

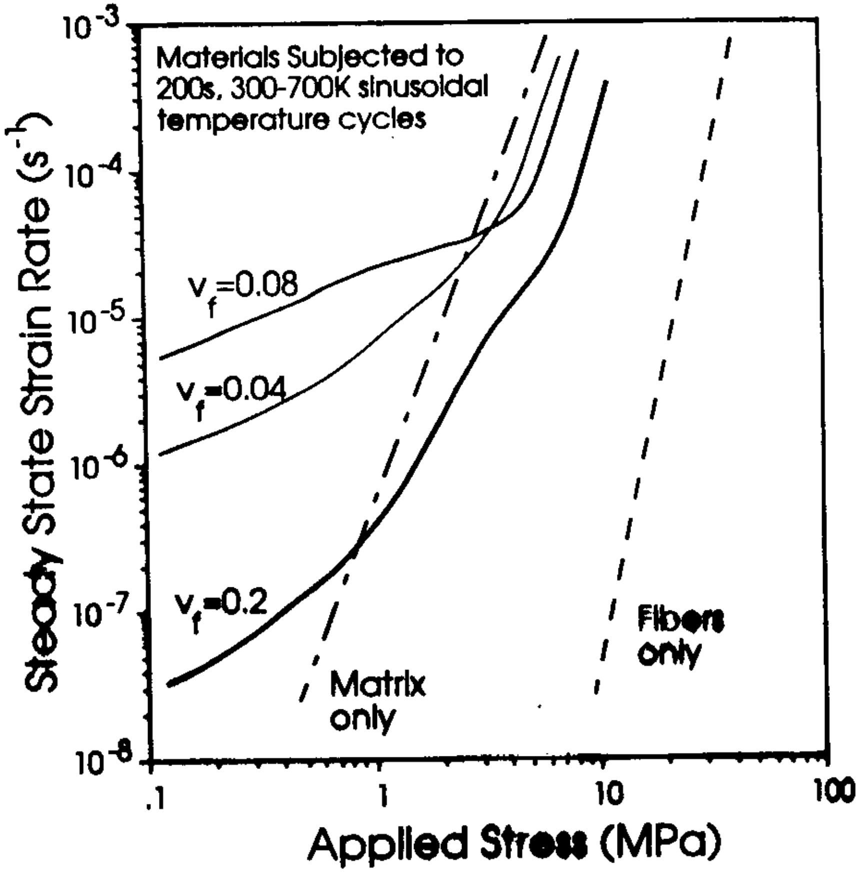

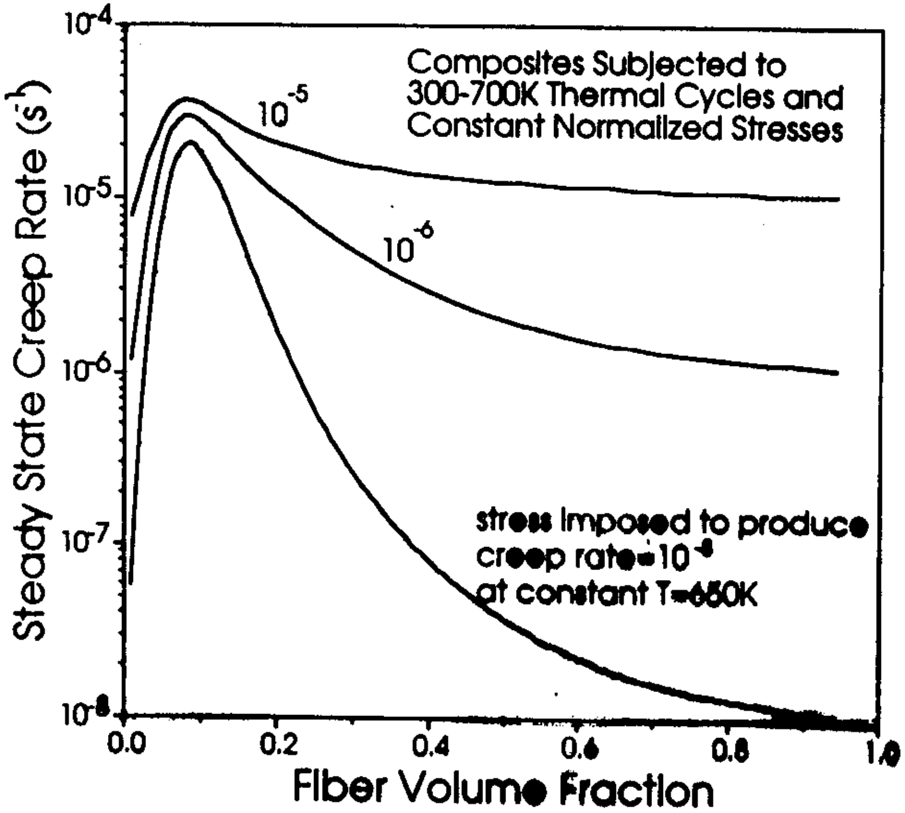

Conclusions:

- Experimental and theoretical evidence have demonstrated that temperature changes have an important influence on the deformation of composite materials.
- These effects should be considered in life prediction regarding composite materials
- These considerations can aid in the design of "good" high temperature composites.
- More work is needed to understand effects of:
  Interface Behavior
  3-D Reinforcement Geometry
  Actual State of Stress
- Some related processes need examination:
  Internal Damage
  Crack Propagation
- The study of model systems and limiting cases represents an important step in understanding these effects.

Conclusion - How to Design a Creep Resistant Material

1) Single Crystal

2) High Elastic Modulus

3) Orient such that Strongest Direction Bears the Load

4) Dispersion Strengthen
-or-
Keep Very Perfect

5) Low Diffusivity (at least for one component)

6) If Second Phase or Composite approach used, assure a small mismatch in Coefficients of Thermal Expansion

- In Press -
~~Submitted to~~ *Metallurgical Transactions*, October 1988

The Deformation of Whisker-Reinforced Metal Matrix Composites Under Changing Temperature Conditions

Glenn S. Daehn
Assistant Professor
Department of Materials Science and Engineering
The Ohio State University
Columbus, Ohio

Gaspar González-Doncel
Research Scientist
Departamento de Metalurgia Física
Centro Nacional De Investigaciones Metalúrgicas (CENIM)
Madrid, Spain

Abstract

A numerical technique for simulating the plastic response of whisker reinforced metal matrix composites under conditions of changing temperature and applied stress is developed. The model simulates an elastic - plastic (diffusion controlled power-law creep) matrix and elastic whiskers, with variable whisker length and spacing. To test this model, the mechanical behavior of a metal matrix composite of 6061 aluminum, reinforced with 20 volume-percent discontinuous, oriented silicon carbide whiskers was studied under conditions of repeated temperature cycling, and isothermal creep. The results of the thermal cycling experiments are compared to those of the model. Both the experiments and the model demonstrate that the composite flow stress may be significantly reduced by thermal cycling (relative to isothermal, elevated temperature behavior) and that under appropriate conditions, the composite strain rate is proportional to the applied stress. Also, agreement between the experimental results and the first-principles model is very good in terms of both magnitude and trends, despite simplifications in the model.

Introduction

Metal, ceramic and intermetallic matrix composites are receiving much attention as potential high temperature materials. However, several studies on metal matrix composites have shown that thermal expansion differences between the matrix and a reinforcing phase can dramatically accelerate deformation[1,2,3]. The key features of the deformation under sufficiently large temperature cycles and low stresses are that: 1) the material will flow at stresses far below the yield stress at the high temperature of the cycle and; 2) At low applied stress the material deforms with a high effective strain rate sensitivity. This gives rise to high tensile elongation as in conventional fine structure superplasticity. At sufficiently high stresses (or imposed strain rate), thermal cycling has very little effect on deformation.

The deformation of composites under thermal cycling conditions may have potential benefits and imposes some limitations. As a benefit, a thermal cycling process may possibly be developed into a useful new technique for the superplastic forming. The apparent drawback to such a process, however, is that the maximum superplastic strain rate appears to be about 10^{-4} s^{-1} [1,2,4], which may be too low for commercial production applications. However, this effect may be useful for some specialized applications. The enhanced composite deformation seen under changing-temperature conditions may prove to be a drawback in many cases. Many advanced composites are now being developed for elevated temperature service[5], and it has been reported that these materials will creep, and exhibit shape instabilities, at unusually low stresses under thermal cycling conditions[6]. It is therefore important to be able to predict how temperature fluctuations will influence the deformation behavior of these materials in service.

This analysis examines how the stress and strain developed by thermal expansion mismatch and temperature change can influence the axial deformation of aligned whisker-reinforced composites. This simplified analysis is intended to elucidate considerations which must be made when predicting service life for composites in changing temperature environments.

Also, the issues considered should have relevance in the design of composites which will resist the problems associated with temperature changes.

Background

Prior Experimental Results

There are two important conditions under which stress and strain can develop within a material, in the absence of any external forces:

1) Phase changes. If a phase change has an accompanying volume change, mismatch stresses and strains are developed at the transformation front;

2) Changing the temperature of a polycrystalline material which has anisotropic coefficients of thermal expansion. For example temperature changes in polycrystalline α-uranium ($\alpha_{[100]}$=26 X 10^{-6}, $\alpha_{[010]}$ = -2.4 X 10^{-6}) and zinc ($\alpha_{[1010]}$= 15 X 10^{-6}, $\alpha_{[0001]}$ = 60 X 10^{-6}) produce mismatch stresses and strains at grain boundaries. Similarly, changing the temperature of a polyphase material (or composite) in which the constituents have different coefficients of thermal expansion will induce interfacial stresses and strains.

The effects of both of these internal stress generating mechanisms on macroscopic deformation behavior has been studied to some degree (reviews of these results have appeared in the superplasticity literature[7-9]). The general scheme of the experiments is to impose an axial load on a sample and produce internal stresses by repeatedly cycling the temperature. In both cases, the deformation behavior is very similar and is schematically illustrated in Figure 1. The generic behavior can be summarized as follows. So long as the internal strain mismatch is large enough to induce plastic strain, at low applied stresses, the strain per thermal cycle will be proportional to the applied stress[2,10-14]. When strain per cycle is proportional to applied stress, under repeated temperature cycling, strain rate is proportional to applied stress (this is equivalent to a strain rate sensitivity exponent of one and high resistance to neck growth is expected). If the applied stress is raised to a sufficiently high value, then the material will behave as it would without internal stress. This transition occurs when the plastic extension of the sample is on the same order as the plastic strain induced by interfacial mismatch. Thus, the practical effects of thermal cycling induced plastic strain are: 1) the material will deform significantly at stresses far below its isothermal yield stress (at the high temperature of the cycle)[2,3,10-13]; and 2) true superplastic behavior, including extremely high tensile ductility, can be obtained due to the high strain rate sensitivity obtained in thermal cycling[12,14,15]. Thus, this phenomenon has been given the names "environmental superplasticity"[7] and "internal stress superplasticity"[1,12].

Since the present treatment is concerned with the thermal cycling behavior of composites, the behavior of materials containing thermal expansion mismatches under thermal cycling conditions are briefly reviewed in the following paragraphs. Most of the early studies on the effects of thermally cycling a polycrystalline material with anisotropic coefficients of thermal expansion were carried out in uranium, and a few other non-cubic metals, in the absence of any externally applied stress[16-20]. The general conclusion of this work was that in random polycrystalline samples, thermal cycling leads to internal plastic deformation, but no macroscopic shape changes. If, however, the sample contains a preferred crystallographic orientation, repeated thermal cycling may lead to changes in the specimen dimensions in the absence of applied stress[21-23].

A few metals were also studied under an applied stress. Lobb, *et. al.*[15] demonstrated that in polycrystalline α-uranium, cycled between 400° C and 600° C, the strain rate (or, equivalently, strain per cycle) is proportional to the applied stress at low applied stresses, and that very high tensile elongations (beyond 430%) can be obtained without necking. Wu *et. al.*[1] showed similar results with polycrystalline zinc under temperature cycling conditions, they also pointed out that strain rate (or strain per cycle) does not vary strongly

with increasing strain (or number of cycles). Daniels[24] examined the thermal cycling plasticity of polycrystalline zinc in cycling between 0° C and -70° C and again found strain rate to be proportional to applied stress. Furthermore, the flow stress was well below the room temperature yield stress. All three of these studies demonstrated that strain rates can be increased by several orders of magnitude by appropriate thermal cycling, at a given stress, relative to the isothermal strain rate at the high temperature of the cycle.

Recently there have been a number of studies on the deformation of Al-SiC composites under thermal cycling conditions. Sherby *et. al.*[2,12,25] have again shown in this system that the strain rate (or strain per cycle) is proportional to applied stress for 100° C to 450° C cycles, and that due to the high effective strain-rate-sensitivity, tensile elongations in excess of 1000% are possible under thermal cycling conditions. This is remarkable considering that these materials typically show isothermal tensile elongations under 20% at 450° C. It was also demonstrated that under these conditions, whiskers may re-orient and align in the direction of flow[2]. Le Flour and Locicero[3] examined a similar composite in the thermal cycling range of 70° C to 200° C. They concluded that very low stresses (about 10% of the isothermal yield stress) can induce significant strain in the composite, under this low temperature cycling.

Existing Models of Thermal Cycling Enhanced Deformation

The Sherby Model

Recently, Sherby *et al.*[1,2,26] performed creep experiments, under conditions of thermal cycling, on polycrystalline zinc, and aluminum reinforced with silicon carbide whiskers. To analyze their results, they developed a model for creep of metals which considers the presence of an internal stress. The model uses the empirical Garofalo creep relation[27] as a starting point;

$$\dot{\epsilon} = \frac{K}{\alpha^n}\frac{D_{eff}}{b^2}\left[\sinh \alpha \frac{\sigma}{E}\right]^n \quad (1)$$

In this relationship: $\dot{\varepsilon}$ is the strain rate, σ is the applied stress, n is the isothermal stress exponent, D_{eff} is the effective diffusion coefficient, E is the Young's modulus, b is the magnitude of the Burgers vector, and K and α are materials constants.

The Garofalo relation was modified in two ways. First, average quantities for D_{eff} and E are calculated for the thermal cycle. To obtain the average effective diffusion coefficient, $\overline{D_{eff}}$, D_{eff} is time-averaged by numerically integrating D_{eff} as a function of temperature over one cycle. An effective temperature is defined as the single temperature which would give the same $\overline{D_{eff}}$ as is obtained by integration. The effective modulus, $\bar{E}$ is taken as the modulus at the effective temperature.

The second step in this model is to make the assumption that: "At any given time during thermal cycling, half of the dislocations are influenced by an internal stress that aids their motion and the remaining half are influenced by an internal stress that opposes their motion."[1] Further, the model assumes that these two groups of dislocations each contribute independently to plastic deformation. Or, defining the internal stress as σ_i,

$$\dot{\varepsilon} = \frac{1}{2}\dot{\varepsilon}^*[f(\sigma+\sigma_i)] + \frac{1}{2}\dot{\varepsilon}^*[f(\sigma-\sigma_i)] \qquad (2)$$

The Garofalo equation, with the average quantities, is used as the functional form for $\dot{\varepsilon}^*$. The resulting relationship gives the same functional form for the stress v. strain-rate relationships as are obtained in thermal cycling experiments. Strain rate is proportional to applied stress, σ_{app}, when the applied stress is small relative to the internal stress, but reduces to the Garofalo relationship at high applied stresses. When the applied stress is much lower than the internal stress, the resulting relationship can be expressed as:

$$\dot{\varepsilon} \approx \frac{nK\bar{D}_{eff}}{b^2}\left(\frac{\sigma_i}{\bar{E}}\right)^{n-1}\left(\frac{\sigma_{app}}{\bar{E}}\right). \qquad (3)$$

This approach has been used by this group to accurately fit and predict the results of their experiments, as well as those of other researchers. There are, however, elements of their model which are not satisfying. First, the state of stress in the matrix is not adequately described by their scalar treatment. Secondly, the mechanistic description of how applied and internal stresses act on individual dislocations is not well developed, and is especially difficult to accept when the internal stress is much greater than the applied stress.

The prediction of creep rates of materials under non-isothermal conditions is also difficult. The use of average quantities for D_{eff}, E and σ_i makes it difficult to predict deformation behavior under wide temperature variations or under the action of one-time transients. Also, in order to predict the thermal cycling creep rate, one must estimate the internal stress for the thermal cycling conditions. The model relates σ_i to the "yield stress" of the material at the effective temperature, and an appropriate strain rate (which is related to the cycling rate). σ_i is difficult to predict with high accuracy under conditions of changing temperature. However, at low applied stress, thermal cycling creep rate is proportional to σ_i raised to the (n-1) power, where n is the isothermal stress exponent (typically 5-20). This makes accurate predictions with this model exceedingly difficult.

Approaches Based on the Levy-vonMises Flow Law

One of the early observations of accelerated deformation because of internal stress was encountered in the creep of polycrystalline orthorhombic α-uranium. When subjected to irradiation by neutrons it was found the creep rate of α-uranium was 1.5 to 2.0 times greater than under normal (non-irradiated) conditions[28]. In single crystals of uranium, the effect of irradiation is to elongate the crystals along the *b* axis and decrease their length along the *a* axis, at a strain rate $\dot{\varepsilon}_g$, which is a function of flux. Internal stresses and strains thus develop at grain boundaries in polycrystalline uranium. This problem was first analyzed by Roberts and Cottrell[29]. They concluded that the intergranular stresses induced plastic flow in the grains, and that most of the work of deformation is done by these internal stresses. The external stress serves to influence the local deformations such that the averaged external strain has a non-vanishing component in the direction of the applied stress. They estimated that the external strain rate, $\dot{\varepsilon}_e$, of the uranium should be on the order of

$$\dot{\varepsilon}_e \approx \left(\frac{\sigma_{app}}{\sigma_y}\right)\dot{\varepsilon}_i \qquad (4)$$

where σ_y and σ_{app} are the material's yield stress and the applied stress, respectively.

Based on this early qualitative work, a number of workers have developed quantitative models of deformation under conditions of internal stress, as produced by: thermal cycling with a thermal expansion mismatch[30,31], radiation growth[30] and repeated phase transformations[4]. All of these models estimate the stress state in an average grain of material. This stress is produced by both the externally applied load and internal stresses. The resulting plastic flow is then resolved by use of the Levy-vonMises flow law[32,33] (This theorem basically states that, for an isotropic material experiencing plastic flow, the plastic strain rate in any direction is proportional to the deviatoric stress in that direction). An important boundary condition in the development of these models is that in the absence of an applied stress, the average of the internal stresses in the material over all grains is zero at any time. Therefore, if no load is applied, the material's shape will not change plastically during thermal cycling. If a material has a load applied which is much less than the yield stress, and the internal stress produces yielding within the material, the average normal stress in the material will be non-zero and there will be an elongation of the material in the direction of the applied load. By these models, the amount of elongation will be proportional to the applied load, the amount of internally-induced plastic deformation, and is inversely proportional to the material's flow stress. Under high applied stresses (i.e. approaching the yield stress), isothermal deformation behavior is approached. Models of this type have been shown able to predict the behavior of metals undergoing an isothermal (or nearly isothermal) phase transition[4]. However, currently they can only be

qualitatively invoked for real materials going through large thermal cycles, since flow stress varies strongly with temperature.

A Model for Composite Deformation

In the following sections, a model is developed to describe the plastic deformation of a whisker reinforced metal matrix composite under changing temperature conditions. This model closely follows a much simpler version proposed earlier[34]. The modeling begins by understanding the stress state in the matrix, between the whiskers. Then using a simple, accepted, constitutive equation, the strain in the matrix can be calculated and related to overall strain in the composite. Since the constitutive equation used is general, the model can be used to predict behavior ranging from isothermal high temperature creep to low temperature thermal cycling. The modeling will use only parameters which can be independently measured in isothermal tests.

Effect of Applied Stress

Consider how plastic deformation may occur in an aligned whisker-reinforced material. The typical situation is to reinforce a ductile matrix with stronger, high aspect ratio whiskers. An idealized geometry is presented in Figure 2. It is clear that even in this simplified geometry the stress state in the matrix of this composite is complex, and dependent upon location (i.e. the stress state in the matrix near the end of a whisker is different than in regions which are constrained between two closely spaced whiskers).

If the assumptions are made that the whiskers do not deform plastically and that there is perfect bonding between the whiskers and the matrix, the only way in which such a composite can sustain significant plastic elongation is if there is shearing of the matrix, between whiskers and accommodation at the whisker ends. The required shear stress in the matrix, between two whiskers, is shown in Figure 2b. Based on these observations, the following geometric assumptions will be incorporated into this model:

- There is perfect bonding between the matrix and whiskers.
- The whiskers have a length, L ,that is much greater than the inter-whisker spacing, S. Whisker end effects are neglected.
- Shearing of the matrix, between whiskers, sets the strength of the composite, and is the rate limiting step in composite deformation.
- The entire applied stress on the composite is transmitted through the reinforcing whiskers which constitute V_w volume fraction of the composite. The matrix has a volume fraction $V_m=1-V_w$.
- Stresses and strains are uniform in the matrix, and the matrix is isotropic.
- Elastic and plastic deformation are permitted in the matrix. Only elastic deformation is permitted in the whiskers. The whiskers are also elastically much stiffer than the matrix.
- A two dimensional problem will be studied.

When these assumptions are incorporated, the composite geometry shown in Figure 3a is obtained. The black lines represent whiskers, and gray denotes matrix. With this assumed geometry, voids will appear in the composite upon deformation, as is illustrated in Figure 3b. Clearly a single, uniform shear strain cannot adequately describe the full state of strain in the matrix of real composites, and other stress and strain states are required near whisker ends. However, the shearing process illustrated in Figure 3b may control the deformation rate in some cases, and this is assumed in this model. This geometric model is attractive since thermal and applied stresses can be resolved as independent axial, and shear components.

The transfer of a load applied to the composite on to the matrix is now examined. A coordinate system based on the transverse, X, and whisker, Y, directions is also indicated. In accord with Figure 3b, the shear stress acting locally on the matrix, τ_{xy}, can be related to the stress externally applied to the composite, σ_{comp} by:

$$\tau_{XY} = \frac{\text{Force}}{\text{Area}} = \frac{S\sigma_{comp}}{\left(\frac{L}{2}\right)} = \left(\frac{2S}{L}\right)\sigma_{comp} \quad (5)$$

The composite plastic elongation, ε_{comp}, can also be related to the plastic shear strain in the matrix, γ_{xy}. Again, referring to Figure 3b, one may see that the relationship is:

$$\varepsilon_{comp} = \left(\frac{2S}{L}\right)V_m\gamma_{XY} \quad (6)$$

Based on this analysis, a geometric factor, F, can be defined as:

$$F = \left(\frac{L}{4S}\right) \quad (7)$$

With this definition, the stress and plastic strain imposed on the composite can be related to that in the matrix in a very simple and useful form:

$$\tau_{XY} = \frac{\sigma_{comp}}{2F} \quad (8)$$

$$\gamma_{XY} = \frac{2F\varepsilon_{comp}}{V_m} \quad (9)$$

These equations intuitively show that if the introduction of whiskers to the matrix will strengthen the composite by some factor, then the strain in the matrix will be amplified by the same factor. These equations are consistent with conservation of energy. The equations developed here are in accord with the more general relationships developed by McLean[35] which describe steady state creep in whisker reinforced composites under isothermal conditions.

Effect Of Temperature Change

The other stress component which requires understanding is the stress generated by the thermal expansion mismatch. Throughout it shall be assumed that there are no temperature gradients through the composite. In the composite, it is assumed that the whiskers and matrix are perfectly bonded at the interface, and the matrix is fully constrained by the whiskers. This requires that through a temperature change the lengths of the matrix and whiskers must remain equal, and tensile forces in one component must be balanced by compressive forces in the other. By these considerations, the axial stress in the matrix can be related to the strain mismatch brought on by a change in temperature of ΔT by:

$$\sigma_Y = -\left[\frac{E_m(\Delta\alpha\Delta T + \varepsilon_Y)}{\left(1 + \frac{V_m E_m}{V_f E_f}\right)}\right]. \qquad (10)$$

In this relationship $\Delta\alpha$ is the difference between the coefficients of thermal expansion for the matrix and whisker. E and V are Young's modulus, and volume fraction, respectively. The subscripts w and m refer to the whisker and matrix, respectively. The term ε_Y represents the amount of axial plastic flow in the matrix resolved in the whisker direction, relative to the initial state.

State of Stress and Strain in the Matrix

Both the thermally generated stress, σ_Y, (Equation 10) and the applied stress component, τ_{XY}, (Equation 8) can be imposed on the matrix as indicated in Figure 4. Note that the thermally generated stress produces only an axial stress, and the applied stress results in a pure shear stress. These matrix stress components can be plotted onto Mohr's circle of stress as shown in Figure 5. The maximum resolved shear stress, τ_{max}, (which is the "effective stress" for plastic flow) and the angle between the plane of maximum shear stress and the whisker direction, θ are given by,

$$\tau_{max} = \sqrt{\tau_{XY}^2 + \left(\frac{\sigma_Y}{2}\right)^2} \qquad (11)$$

$$2\theta = \arctan\left(\frac{\sigma_Y}{2\tau_{XY}}\right) \qquad (12)$$

If a small of plastic strain increment, $\Delta\gamma$, (an effective plastic strain increment) is now allowed, this plastic shear strain will occur on planes of maximum shear stress. Mohr's circle of strain, shown in Figure 6, is now used to resolve the shear strain back onto the X-Y coordinate system. The diameter of the

circle is $\Delta\gamma$, and the angle between the whisker direction and planes of maximum shear stress, θ, has been set in Equation 12. On the X-Y coordinate system,two strain components can be resolved as a shearing between whiskers γ_{xy} and an axial strain ε_y:

$$\gamma_{XY} = \Delta\gamma \cos 2\theta \qquad (13)$$

$$\varepsilon_Y = \left(\frac{\Delta\gamma}{2}\right)\sin 2\theta. \qquad (14)$$

When Equation 14 is substituted into these equations, they can be simplified to:

$$\gamma_{XY} = \Delta\gamma\left(\frac{\tau_{XY}}{\tau_{max}}\right) \qquad (15)$$

$$\varepsilon_Y = \Delta\gamma\left(\frac{\sigma_Y}{4\tau_{max}}\right). \qquad (16)$$

Again, the strain component ε_y serves to decrease the thermally induced stress, while γ_{xy} elongates the sample in response to the applied load. Considering Equation 9, the plastic elongation of the composite can be related to the stress and strain in the matrix, during the strain increment, by:

$$\varepsilon_{comp} = \Delta\gamma\left(\frac{\tau_{XY}}{\tau_{max}}\right)\left(\frac{V_m}{2F}\right) \qquad (17)$$

Matrix Constitutive Behavior

A relationship between the matrix strain-rate and current values of stress, temperature and prior strain, is required to model deformation of the idealized composite. Real matrix behavior is very complex under the circumstances to be modeled. Whiskers contribute dispersion hardening and stabilize small subgrains. The widely varying temperature and stress state further complicate the situation. For these reasons, the simplest, justifiable matrix behavior is assumed for this model: diffusion controlled power-law creep, with no strain hardening effects. Other flow rules may can work as well or better, but this flow rule incorporates a wide range of behavior and has a physical basis.

Specifically, the assumed relationship between the shear (effective) strain rate and the shear (effective) stress is:

$$\dot{\gamma}_{max} = K D_{eff} \tau^{n}_{max} \qquad (18)$$

where τ_{max} is the maximum resolved shear stress. $\dot{\gamma}_{max}$ is the plastic shear strain rate resolved on planes of maximum shear stress. K is a material constant which relates to strength. n is the stress exponent and D_{eff} is the effective diffusion coefficient. D_{eff} represents the diffusion coefficient which is the sum of terms for lattice and pipe diffusion and can be represented by;[36]

$$D_{eff} = D_{ol} \exp\left(\frac{-Q_l}{RT}\right) + 320\left(\frac{\tau_{max}}{E}\right)^2 D_{op} \exp\left(\frac{-Q_p}{RT}\right) \qquad (19)$$

where D_{ol} and D_{op} are pre-exponential constants, Q_l and Q_p are the activation energies for diffusion. The subscripts l and p refer to lattice and dislocation pipe diffusion, respectively. R is the gas constant and T is the absolute temperature. The dislocation density varies with the state of stress in the material, therefore the pipe diffusion coefficient also varies with stress.

Computational Technique

All the elements necessary to simulate plasticity of whisker reinforced metal matrix composites under thermal cycling conditions have been presented. Based on these equations, a computer program for simulating the behavior of the metal-matrix composite has been written. The essence of the program is shown in Figure 7 and is described in the following paragraph.

Initially the composite begins at the low temperature of a thermal cycle. The applied stress on the composite provides a shear stress in the matrix. No other internal stresses or strains are present. When the simulation begins a short time interval, Δt, progresses, and the temperature of the composite changes by a small amount. The applied load generates a shear stress (Equation 9), and the thermally generated (axial) stress is determined (Equation 10). The direction and magnitude of the maximum shear stress is calculated (Equation 11). Plastic flow is permitted along planes of maximum shear stress for a short time interval, as governed by a constitutive equation

(Equation 18) which considers the current state of stress and temperature. The plastic strain which took place during the time interval ($\dot{\gamma}\,\Delta t$) is resolved as shear and axial strain onto axes defined by the X-Y coordinate system (Equations 15 and 16). These plastic strains are added to their current values and provide ε_y and γ_{xy} as time progresses. This procedure is repeated for each short time increment.

Experimental Procedures

The material chosen for the experimental part of this study is a metal-matrix composite consisting of a 6061 aluminum alloy reinforced with 20 volume-percent silicon carbide whiskers which was prepared by powder metallurgy techniques. The whiskers have a mean diameter slightly less than 1μm, and lengths on the order of 10μm. The composite was consolidated by back extrusion of a tube 152.5 mm in diameter and 12.7 mm in wall thickness. as a result of this process, the whiskers are strongly oriented in a plane parallel to the extrusion direction, and are weakly oriented in the extrusion direction.

Test specimens were prepared with the tensile axis parallel (longitudinal samples) and perpendicular (transverse samples) to the extrusion direction. The samples have cylindrical gage sections of 5.08 mm in length and 2.54 mm in diameter. This geometry was utilized for both thermal cycling creep tests and strain-rate-change tests at constant temperature (isothermal tests). In this investigation, both longitudinal and transverse samples were tested under isothermal conditions and only longitudinal samples were tested under temperature cycling conditions.

Isothermal tensile strain-rate-change creep data was taken in longitudinally and transversely oriented samples with a Instron load frame at 723 K. Heating was provided by a dual elliptical radiant quartz furnace, and the temperature was maintained within 2° C. The stress v. strain rate relationship was determined by elongating the sample 3 to 5% at one cross-head speed and increasing the cross-head speed by about a factor of three and elongating the sample another 3 to 5%. This procedure was repeated increasing the strain rate each time until approximately three orders of magnitude in strain rate were covered. In each rate segment, the flow stress came to a plateau value.

Thermal cycling experiments were performed on longitudinally oriented cylindrical samples in tension. Two series of experiments were run. One examined the relationship between strain-rate and applied stress, at fixed temperature cycling conditions. Another series of experiments examined the effect of the amplitude of the temperature cycle on deformation rate, at a fixed applied stress. For both series of experiments, the equipment used was similar to that used by Wu *et. al.*[1], and consisted of a quartz radiant tube furnace, temperature controller and a load train that included a constant stress cam. The temperature was measured by a thermocouple which was embedded in a hole in the top of the sample. Thermal cycling was achieved by a system of relays and timers. Specifically, the furnace operated until a pre-set high temperature is reached. At this point the furnace switches off and the sample is cooled by forced convection until a programmed time interval elapses. Then, the timer re-sets and the furnace heats again. Thus, the upper temperature of the cycle and the cycle period were controlled directly. The lower cycle temperature is indirectly controlled by controlling the heating rate, cooling rate and cycle time. Strain rate was obtained by dividing the sample strain (calculated based on the sample's reduction in area), by the total time of testing under thermal cycling conditions. In all cases, there was a linear relationship between strain and time (or number of temperature cycles).

The relationship between applied stress and strain-rate was determined by setting a 200 second cycle between 373 K and 723 K, and applying varied stresses. In cycling, approximately 140 seconds was required for heating and 60 seconds for cooling. One set of data was obtained by applying a different stress to separate samples and straining them to high elongation (>30%).

Another set of data was obtained by using one sample and varying stress, and measuring the strain rate, only allowing 3 to 5% strain at each stress level.

The effect of thermal cycle amplitude was explored in another series of experiments. Longitudinally oriented composites were studied at a constant stress of 10 MPa. The amplitude of the temperature cycles was varied by decreasing the lower cycle temperature. The high temperature was maintained at 723 K. To accommodate the largest possible range of thermal cycling amplitudes, two cycle periods were used. A 90 second cycle was used for the smallest thermal cycles (678 K-723 K through 257 K-723 K). And a 200 second cycle was used for the larger thermal cycles (606 K-723 K through 228 K-723 K). The cycle sizes were varied by changing the heating and cooling rates. The smallest cycles were attained by insulating the furnace. Faster cooling rates were achieved through forced-air cooling. The largest cycle (228 K-723 K) was achieved by cooling with a liquid nitrogen mist. One sample was used in these experiments. A few percent strain in each cycling condition was used to determine strain rate.

Results and Analysis

Determination of Constants

The first task in predicting deformation behavior is to identify appropriate constants for the model. The aluminum diffusion constants[37-39]; and values for the moduli of the silicon carbide[40] and the aluminum[41] and thermal expansion constants[42,43] for both materials were taken from the literature. These data are presented in Table I.

The matrix stress v. strain-rate relationship as well as the geometric factor, F, can be estimated from the 723 K isothermal strain-rate-change tests on the longitudinal and transverse samples. These data are shown in Figure 8. From these data, the independent contributions of geometric strengthening and matrix strength must be determined. One must realize that the introduction of whiskers into a matrix strengthens the resulting composite in two independent ways: 1) Whiskers inhibit the motion of dislocations directly, and by stabilizing small subgrains (i.e. they effectively strengthen the matrix by refinement). This effect is independent of composite orientation; 2) As discussed previously, the whiskers change the way in which the composite may deform. The whiskers bear a large part of the stress. Therefore, stress and strain locally in the matrix are no longer equal to the stress and strain macroscopically imposed on the composite. The magnitude of this geometric strengthening is a function of composite orientation.

Since in a real composite there is a complex distribution of whisker sizes and inter-whisker spacings, and slip will generally occur where easiest, effective values of S and L (in the context of Equation 7) are needed to define F. In this analysis it is assumed that the matrix stress v. strain-rate behavior can be approximated by the the composite when tested in the transverse orientation (i.e. F=1 in this orientation), since whiskers which are perpendicular to the testing axis cannot bear any load. While this assumption is not strictly correct, it is a useful one, and the error it introduces is discussed later. Thus, K and n in the constitutive law, Equation 18, can be set based on the transverse tensile data, and are shown in Table I. Since the matrix behavior is assumed to be represented by the transverse stress v. strain rate relationship, in a composite with a reinforcement factor of F, the same state of stress and strain rate in the matrix will exhibit a macroscopic composite flow stress a F times greater, and a strain rate which is decreased by a factor of F/V_m. These relationships come directly from Equations 8 and 9. In applying this reasoning to Figure 8, a F of 1.2 can be estimated for the longitudinally oriented composite. This is a reasonable approximation. A close packed array of 10μm long, 1μm diameter whiskers, which comprise 20 volume percent has an inter-whisker spacing of about 2.0μm. Therefore F as calculated by Equation 7 is about 1.25.

Predicted Composite Behavior and Comparison to Data

The constants presented in Table 1 were used with the model and predictions were made regarding deformation of the 6061Al-20% SiC_w composite under thermal cycling conditions. These were compared directly to the thermal cycling data obtained experimentally.

Stress and Strain vs. Time

Figure 9 shows the type of behavior, in terms of stress and strain as a function of time, which are available from this model. These simulations were run under imposed axial stresses on the composite, σ_{comp}, of 5 MPa and 20 MPa. Figure 10a shows the sinusoidal temperature variation which was used in modeling. The cycle is varies from 373 K to 723 K with a 200 second period.

The temperature change produces a normal stress in the matrix. This stress, σ_y, is plotted as a function of time in Figure 9b. Since the model incorporates the temperature dependance of flow stress, the magnitude of the σ_y increases throughout cooling, but eventually decreases upon increasing temperature. It is also noteworthy that changes in the applied stress serve to change the thermally induced stress slightly. This occurs because the full state of stress in the matrix is estimated.

The components of plastic strain as a function of time are plotted in Figure 9c. The axial strain components at 5 and 20 MPa are shown on the bottom part of the figure. Again, variations in the applied stress have little effect on these strain components. The upper curves show the plastic elongation of the composite as time progresses. The slope of this line over several cycles gives the steady state strain rate of the composite. Examination of these curves shows that in this range, the composite strain rate is approximately proportional to the applied stress and that significant composite elongation only occurs when plastic flow is being induced by changing temperature.

The predictions in Figure 9c only represent the effects of plastic elongation, which occurs by shearing of the matrix elements. The composite length may also change by thermal expansion. However, as analyzed by Garmong[44], elastic, plastic, and thermal expansion strains must be coupled in these composite systems. Continuing with the assumption that there is perfect bonding at the whisker / matrix interface, the lengths of the whiskers and matrix elements must remain equal. Therefore, the total axial strain in the composite, ε^T, is given by the sum of the reversible elongation (thermal and elastic) of the whiskers (which is equal to that for the matrix) and the plastic elongation of the composite. This is given by:

$$\varepsilon^T = \varepsilon_{Comp} + \alpha_f(\Delta T) + \left(\frac{\Delta\sigma^{whis}}{E_f}\right) \tag{20}$$

ε_{comp} is defined in Equation 17. $\Delta\sigma^{whis}$ refers to the change in the axial stress in the whisker, relative to that which would be present under load but without any thermally induced internal stresses. This can be related to the matrix stress by the isostrain rule of mixtures as:

$$\Delta\sigma^{whis} = \frac{-V_m \sigma_Y^{matrix}}{V_f} \tag{21}$$

σ_Y^{matrix} is defined by Equation 10.

The total composite axial elongation is plotted as a function of time with applied stresses of 5 and 20 MPa in Figure 10a. This figure shows that thermal expansion is generally the dominant term for a single thermal cycle. However, the applied stress also leads to composite elongation, and the elongation rate is roughly proportional to the applied stress.

Another interesting feature of this analysis is that if the plastic elongation of the composite elongation is neglected (i.e. only the last two terms of Equation 20 are considered), there is a hysterisis in the relationship between composite strain and temperature. This is illustrated in Figure 10b. This hysterisis will exist regardless of applied stress. However, its magnitude

may be affected somewhat. This effect was analyzed in a similar manner by Garmong[44] and this prediction shows the same features as experimentally measured length v. temperature curves for composite materials[45].

Effect of Applied Stress

The strain rates obtained from 6061Al-20% SiC_w composite cycled between 373 K and 723 K at various applied stress levels are shown in Figure 11. To model the stress v. strain-rate behavior, a sinusoidal temperature with the same amplitude and period was used with the model, and the steady state composite strain rate was calculated at several imposed stresses. This predicted applied stress stress (σ_{comp}) v. strain rate ($\dot{\varepsilon}_{comp}$) relationship is also plotted in Figure 11. The creep rate of the metal-matrix composite in the absence of an internal stress has also been predicted and is presented in Figure 11. This relationship was developed by setting the difference between the coefficients of thermal expansion between the whiskers and matrix to zero ($\Delta\alpha$=0). Therefore, no thermal stress σ_Y, could develop in the composite. Running the simulation then gave the isothermal creep rate as time averaged at each temperature at the applied stress. This is equivalent to the isothermal composite creep rate at the "effective temperature" as defined by Sherby and co-workers[1].

The figure shows the predicted thermal cycling stress v. strain-rate behavior for the metal matrix composites has the same characteristics as have been seen experimentally. The steady state creep rate has a strain-rate-sensitivity exponent approaching 1 at low stress. The creep rate approaches the effective isothermal behavior at high stress. And, most importantly, the predicted behavior corresponds to the experimentally observed behavior within the experimental error in the strain-rate measurements. This suggests the proposed model may accurately predict deformation under non-isothermal conditions.

Under these temperature cycling conditions and low stresses the high strain-rate-sensitivity-exponent inhibits neck growth and allows extremely high tensile elongations. At 623 K and strain rates on the order of 10^{-3} s^{-1} this composite fails at less than 10% elongation. Under temperature cycling, the Al-SiC_w composite reached elongations to failure of 12%, 600%, and 1050% at respective applied stresses of 40 MPa, 20 MPa and 10 MPa. This is consistent with the increase in the strain-rate-sensitivity-exponent with decreasing applied stress.

Effect Of Thermal Cycle Amplitude

Another important issue is how the amplitude of thermal cycles will affect creep rate. This effect may be important in the life prediction of metal-matrix composites under non-isothermal conditions. Furthermore, this understanding can aid in the determination of what accuracy in temperature control is needed to acquire "isothermal" creep data when testing metal-matrix composites.

To address these issues the model was run to simulate the conditions of the experiments run with varied temperature cycle amplitudes. In modeling, the sinusoidal thermal cycle was imposed on the composite, with 200 and 90 second periods. The high temperature of the cycle was maintained at 732 K, but the lower temperature was varied. The resulting predictions and experimental results at 10 MPa applied stress are shown in Figure 12. More than one order of magnitude in both temperature cycle amplitude and strain rate were experimentally examined. Furthermore, since the power-law creep relationship is well accepted, this prediction is also expected to be good at very small temperature cycle amplitudes. Thus, the predictions and the experimental data are in good agreement. These data, and the data shown in the last section, strongly support the proposed model for thermal cycling plasticity in metal matrix composites.

The shape of the predicted relationship between cycle amplitude and strain-rate requires some explanation. At low cycle amplitudes, the thermal cycling creep rate approaches the isothermal creep rate. The deformation rate is not strongly affected until the thermally induced stress is on the order of

the applied stress. Upon increasing the thermal cycle amplitude, the thermal cycling creep rate does not significantly increase until the thermally generated stress becomes similar to the applied stress. As the thermal cycling amplitude increases, the composite creep rate is driven strongly by the imposed temperature changes. For large cycles most of the work of deformation is done by the thermally induced stress and the applied stress merely influences the resolution of the strains. At very large thermal cycles, the slope of the strain rate v. thermal cycle amplitude curve begins to decrease. This can be understood by recalling that these curves were generated by fixing the high temperature and cycling to lower low temperatures. Thus, the material strength (averaged over the cycle) increases as the amplitude of the temperature cycles increases. As was shown in Equations 4 and 17, at any particular time, the composite strain (with applied stress held constant) is inversely proportional to the matrix flow stress. Thus, little elongation is obtained in the low temperature part of the cycle where the matrix flow stress is high. Conversely, if the low temperature were fixed and larger cycles were achieved by using higher high temperatures, the slope of the strain rate v. cycle amplitude curve would continue to increase, since the average matrix flow stress would continue to decrease.

Figure 13 shows the predicted effect of different applied stresses on the temperature cycle amplitude v. strain rate relationship. The most striking aspect of this figure is that the curves generated at 5, 10 and 20 MPa are well separated at low cycle amplitudes, but become very close together at high stress amplitudes. This is an expression of the stress exponent being high in isothermal conditions, and low under thermal cycling conditions. Note that the magnitudes of temperature cycle amplitudes needed to double the cycling rates are approximately 3 K, 6 K and 12 K, at 5 MPa, 10 MPa and 20 MPa, respectively. This again demonstrates that deformation will be accelerated when the thermally induced stress is of the same order of magnitude as the applied stress. This figure also clearly shows that composite behavior at low stress is very strongly affected by temperature fluctuations.

Discussion

A first-order model for the analysis of deformation in polyphase materials under thermal cycling conditions has been developed. This model allows the straightforward examination of how microstructural and thermal-cycling variables can influence deformation. Despite geometric simplifications, the model has been shown to agree with experimental data with reasonable accuracy and no serious discrepancies between the predicted and the experimentally observed thermal cycling behavior were found. Thus, this new model seems to have real predictive capability. The important open question is: is the model valid? To make the problem tractable and more intuitively clear, some gross simplifications were made. Specifically, there were two important simplifications in the model development. First, in real composite materials, the state of stress and strain in the entire matrix cannot be characterized by one representative element. Secondly, it is not yet clear that the geometric factor "F", which was developed in two dimensions, has relevance in real composite materials. These issues will be addressed in turn.

In real composite materials, stress and strain in the matrix cannot be resolved into two independent shear and axial components which relate to composite elongation and shear, respectively. Stress and strain in the matrix have a complex spatial variation which cannot be simply characterized. It is suggested that the important accomplishments of the current method are that it estimates, with reasonable accuracy, the effective plastic strain induced in the matrix with each temperature cycle, and the effective stresses and strains involved in composite elongation are also estimated in a reasonable way. Recall that a key result of the previous Levy-vonMises based analyses of related problems is that elongation per cycle (at fixed applied stress) is proportional to the amount of plastic strain per cycle and inversely proportional to the material flow stress. In summary, the key to the physical process is that: temperature cycling induces some amount of plastic deformation in the matrix; this strain would be fully reversed with each cycle if no external stress were imposed, but with stress applied, the matrix strains irreversibly in response. Therefore the model is predictive, not because it precisely describes the state of stress in the matrix, but because it estimates the effective thermally-induced plastic strain and accounts for the applied stress in a reasonable manner.

The relationship between the applied stress and the stress which acts on the matrix is the other major assumption of this model. The need for a term like "F" is justified by the fact that the flow stress of whisker reinforced composites varies with the testing axis. If the matrix is assumed to be isotropic, it follows that the whisker alignment and distribution will influence the stress transmitted to the matrix. A geometric term is also important since it influences the transition-strain-rate between low stress-exponent and high stress-exponent behavior. Assuming a fixed amount of thermally induced plastic strain per cycle, the transition rate will be proportional to $1/F$. In the current analysis, the assumption that $F=1$ for the composite oriented in the transverse orientation is certainly not strictly true (but this error is probably small). However, this will not produce a large error in the model, since the creep constant, K, and F must be set together based on longitudinal creep data. (Thus, at high applied stresses, the thermal cycling creep rate matches that which would result without any internal stresses). Thus, if "F" is estimated as being 50% too low, the strain rate will be predicted to be 50% too high, at most. Therefore, the predicted deformation behavior is only weakly dependent on F. By this argument, one would expect that loading along other axes (i.e. transverse) will have relatively little effect on strain rate under thermal cycling conditions. This has been shown experimentally by Hong *et. al.*[2].

The assumed constitutive law is also somewhat oversimplistic. The model essentially uses steady state creep data to set the stress v. strain-rate behavior of the matrix. When effect of directional hardening (which has little effect in the thermal cycling case, but is an important factor in steady state creep measurements) is considered, the effective strength of the matrix is lowered. Therefore, the amount of thermally induced effective plastic strain in the matrix is underestimated by this model. On this basis it is expected that the model may underestimate the composite strain rate slightly. This could be corrected if the matrix constitutive behavior in these composites were understood more fully.

Concluding Remarks

A simplified, first principles model for modeling deformation in metal matrix composites under conditions of temperature change has been presented. The key elements of the model are a temperature and strain rate sensitive constitutive equation for the matrix material, and a simplified geometric formulation. This model is capable of analyzing the full range of composite deformation behavior, ranging from large thermal cycles to isothermal creep. Furthermore, the model allows time-based analysis of the stresses and strains which act within composites when subjected to temperature changes. The results of this model have been shown to be consistent with a wide range of experimental data. This agreement is in spite of over-simplification with regard to the state of stress and strain in the matrix. The good comparison between theory and experiment suggests that the most important factors in composite deformation under large temperature cycles are: the amount of thermally induced plastic deformation, and the ratio of the current flow stress and the applied stress. The reinforcement geometry is not a large factor, so long as the entire matrix is experiencing thermally induced plastic flow in a fairly uniform way.

The utility of models of this type is that they allows a systematic analysis of how relevant variables (applied stress, temperature cycle amplitude and period, reinforcement geometry, thermal expansion coefficients, elastic moduli, matrix constitutive behavior, etc.) will effect the deformation under conditions where there temperature changes with time. Thus, this approach may be useful in life prediction methodology and materials design related to composite materials.

Nomenclature

Stress and Strain

σ_j - normal stress
τ_{ij} - shear stress
ε_j - normal plastic strain
γ_{ij} - shear plastic strain
$\dot{\varepsilon}_j$ - normal plastic strain rate
ε^T - total elongation of composite
$\dot{\gamma}_{ij}$ - shear strain rate
$\Delta\gamma$ - strain increment, as resolved in maximum orientation
θ - angle between Y axis and maximum shear direction
$\Delta\sigma$ - change in whisker stress due to temperature change

Subscripts
Y - whisker direction
X - transverse direction
max - in maximum orientation
comp - for the composite

Materials Constants - for Matrix and Whisker

E - Young's modulus
α - coefficient of thermal expansion
$\Delta\alpha$ - difference in α_f and α_m
V - volume fraction
F - composite geometric factor (related to whisker spacing/length)

Subscripts
w - of the whisker
m - of the matrix

Matrix Plasticity

K - a creep constant
n - the stress exponent
D_{eff} - the effective diffusion coefficient

Test Parameters

t - time
Δt - a short time increment
T - temperature

Acknowledgements

Support from the ONR Contract #N-0014-82-K-0314 and Prof. Oleg D. Sherby allowed the completion of the experimental work at Stanford University. Support by an Ohio State University seed grant aided one of the authors (GSD) with the completion of this work.

References

1. M. Y. Wu, J. Wadsworth, and O. D. Sherby: *Metall. Trans*, 1987, vol. 18A, pp. 451-462.

2. S. H. Hong, O. D. Sherby, A. P. Divetcha, S. D. Karmarkar, and B. A. MacDonald: *J. Compos. Mater.*, 1988, vol 22. pp. 102-123.

3. J. C. Le Flour and R. Locicero: *Scripta Metall.*, 1987, vol. 21, pp. 1071-76.

4. G. W. Greenwood and R. H. Johnson: *Proc. Roy. Soc. A*, 1965, vol. 283, pp. 403-422.

5. F. D. Lemkey, H. E. Cline and M. McLean (eds.): *M. R. S. Symposia Proceedings--In Situ Composites IV.*, Elsevier Publishing, New York, 1982.

6. G. Garmong and C.G. Rhodes: *Proc. of Conf. on In-Situ Composites, vol. I*, National Acadamey of Sciences, 1973, p. 251.

7. K. A. Padmanabhan and G. J. Davies: *Superplasticity*, Springer-Verlag, 1980, pp. 201-225.

8. J. W. Edington, N. K. Melton and C. P. Cutler: *Prog. in Mat. Sci.*, 1976, vol 21, pp. 61-158.

9. R. H. Johnson: *Metall Rev.*, 1970, Review no. 146, pp. 115-134.

10. F. W. Clinard and O. D. Sherby: *Acta Metall.*, 1964, vol. 12, pp. 911-919.

11. E. Gautier, A. Simon, and G. Beck: *Acta Metall.*, 1987, vol. 35, pp. 1367-1375.

12. M. Y. Wu and O. D. Sherby: *Scripta Met.*, 1984, vol. 18, pp. 773-776.

13. S. T. Kenobeevsky, N. F. Pravdyk and V. I. Kutaistev: *Geneva Conf. on Atomic Energy*, paper no. 681, 1955.

14. R. Kot and V. Weiss: *Metall. Trans.*, 1970, vol. 1, p. 2685-2693.

15. R. C. Lobb, E. C. Sykes and R. H. Johnson: *Metal Sci.J.*, 1972, vol. 6, pp. 33-39

16. S. T. Zegler, R. M. Mayfield and M. H. Mueller: *Trans ASM*, 1958, vol. 50, pp. 905-925.

17. R. M. Mayfield: *Trans ASM*, 1958, vol. 50, pp. 926-942.

18. J. E. Burke and A. M. Turkalo: *Trans ASM*, 1958, vol. 50, pp. 943-953.

19. L. T. Lloyd and R. M. Mayfield: *Trans ASM*, 1958, vol. 50, pp. 954-980.

20. W. Boas and R. W. K. Honeycombe: *Proc Roy Soc, Series A*, 1946, vol. 186, pp. 57-71.

21. R. W. K. Honeycombe: *Deformation in Metals*, Edward Arnold, London, 1984, pp. 349-353

22. J. E. Burke and A. M. Turkalò: *Journal of Metals*, 1952, vol 4, pp. 651-656.

23. S. F. Pugh: *J. Inst Met.*, 1957, vol. 86, pp.497-503.

24. S. Daniels: Master's Research Report, Stanford University, 1985.

25. G. González, S. D. Karmarkar and A. P. Divecha and O. D Sherby: in press, *Composites Science and Technology* .

26. M. Y. Wu: PhD Thesis, Stanford University, 1984.

27. F. Garofalo: *Trans ASM-AIME*, 1963, vol. 227, p. 351-356.

28. S. T. Kenobeevsky, N. F. Pravdyk, and V. I. Kutaistev: *Geneva Conf. on Atomic Energy*, paper no. 681, 1955.

29. A. C. Roberts and A. H. Cottrell: *Phil. Mag.*, 1956, vol. 1, p. 711-717.

30. R. G. Anderson and J. F. W. Bishop: *Institute of Metals Symposium on Uranium and Graphite*, pp. 17-23, The Institute of Metals, 1962.

31. W. S. Blackburn, G. Harnby and J. J. Stobo: *J. Nuc. Energy*, PartA, 1960, vol. 12, pp. 162-171.

32. M. Levy: Compt. Rend. *Acad. Sci. Paris*, 1870, vol. 70, p.1323.

33. R. vonMises: *Gottinger Nachr. Math. Phys. Klasse*, 1913, p. 582.

34. G. S. Daehn and T. Oyama: *Scripta Metall*, 1988, vol. 22, pp. 1097-1102.

35. D. McLean: *J. Mat. Sci.*, 1972, vol. 7, pp. 98-104.

36. H. Luthy, A. K. Miller and O. D. Sherby: *Acta. Metall.*, 1980, vol. 28, p. 169-178.

37. T. S. Lundy, J. F. Murdock: *J. Apl. Phys.*, 1962, vol. 33, p. 1671-1673.

38. M. Beyeler and Y. Adda: *J. Phys.*, 1968, vol. 29, p. 345.

39. T. E. Volin, K. H. Lie and R. W. Balluffi: *Acta. Metall.*, 1971, vol. 19, p. 263-274.

40. P. M. Sargent and M. F. Ashby: *Scripta Metall.*, vol. 17, p. 951-957.

41. W. Koster: *Ziet Metall.*, 1948, vol. 39, p. 1.

42. *CRC Handbook of Chemistry and Physics*, 61st Edition, CRC Press, 1980.

43. A. Taylor, R. M. Jones, J. R. O'Connor and J. Smiltens (eds.): *Silicon Carbide*, Permagon, Oxford, p 147, 1960.

44. G. Garmong: *Metall. Trans.*, 1974, vol 5, pp. 2183-2190.

45. G. Garmong: *Metall. Trans.*, 1974, vol. 5, pp. 2191-2197.

Table I. Constants used in simulation of MMC Deformation

Aluminum Diffusion Data

D_{ol} (m^2/s)	D_{op} (m^2/s)	Q_l (KJ/mole)	Q_p (KJ/mole)
1.7×10^{-4}	2.8×10^{-6}	142	82

Composite Creep Constants & Geometric Factor

Material	n	K	F
6061-20% SiC	11	1.07×10^{-3}	1.2

Component Physical Properties

Component	E (MPa)	α (C^{-1})	Vol Fract
Al	55,000	24×10^{-6}	0.8
SiC	510,000	4.6×10^{-6}	0.2

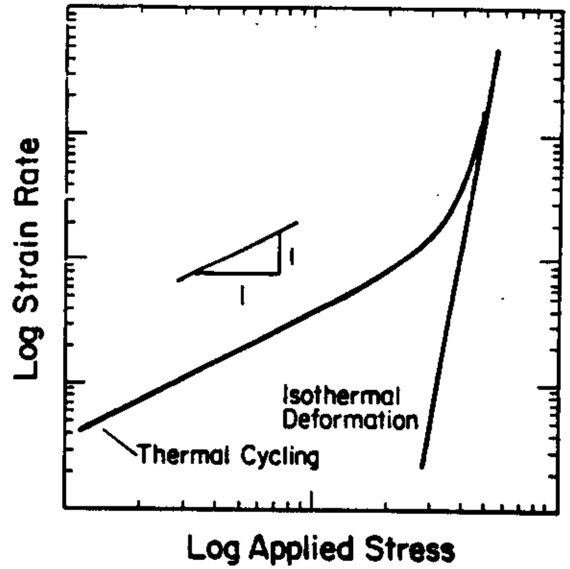

Figure 1. Schematic diagram of the relationship between applied stress and strain rate for materials with large internal strain mismatch under repeated temperature cycling. Note that at low applied stresses, thermal cycling induces a strain-rate-sensitivity-exponent of one and the strain rate is greatly increased relative to isothermal behavior at the same stress. At high applied stresses the internally generated stresses have relatively little effect.

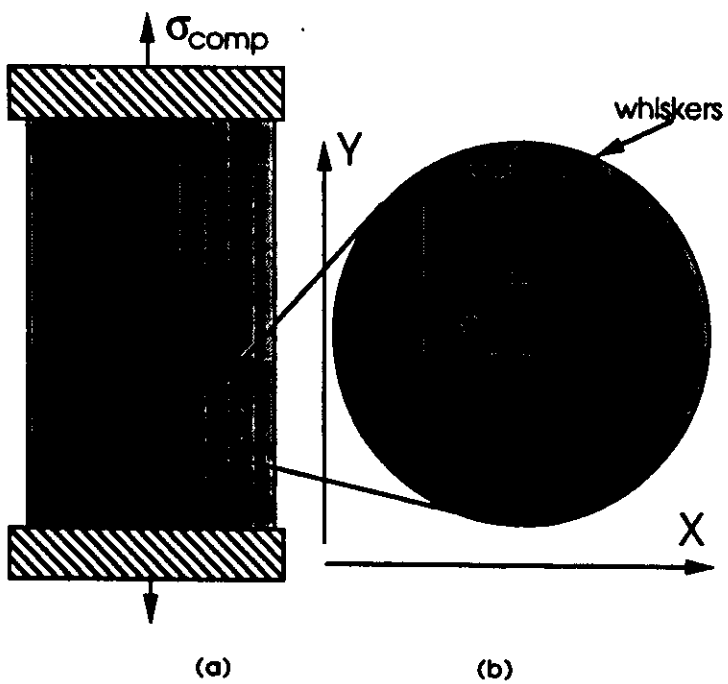

Figure 2. Idealized Composite Geometry, with X-Y coordinate system shown. The prevailing state of stress in the matrix, when constrained between two closely spaced whiskers is shown in (b).

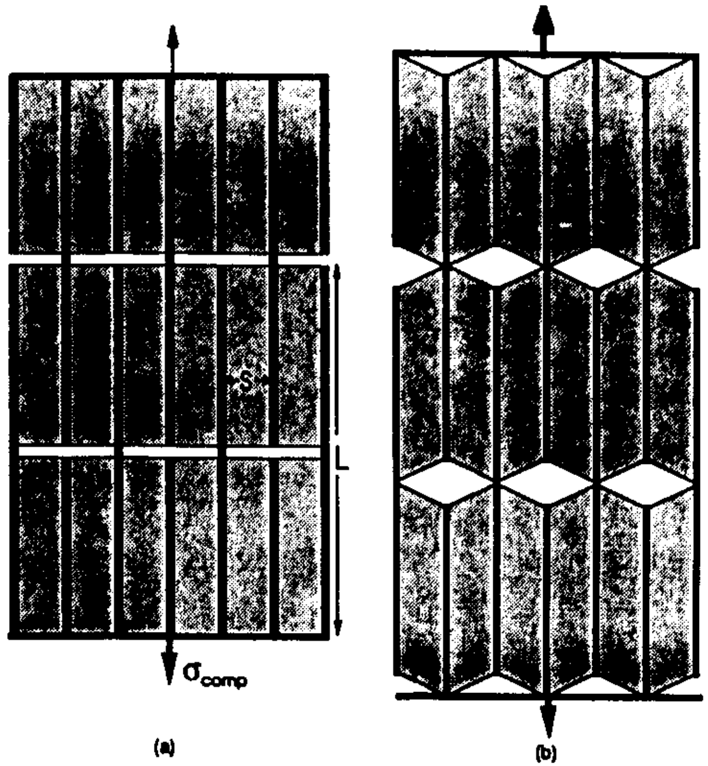

Figure 3. Assumed composite geometry a) unstrained; b) after composite elongation.

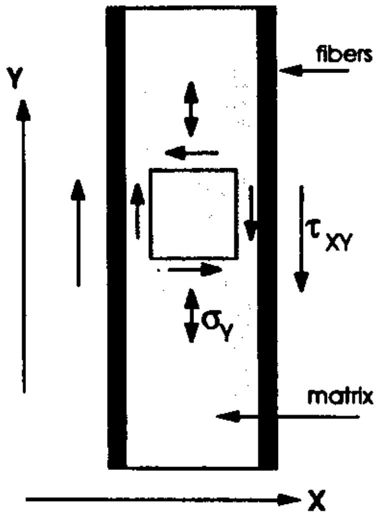

Figure 4. Schematic diagram of the stress state in the matrix. Y and X denote the whisker and transverse directions, respectively.

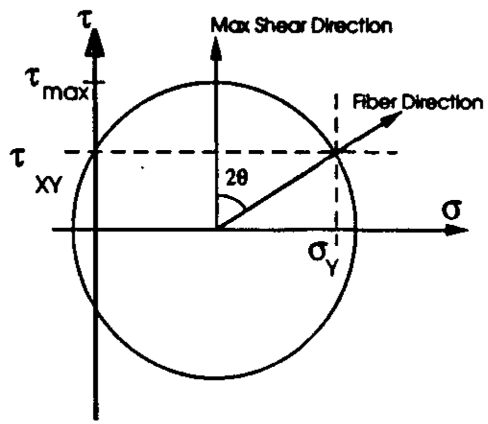

Figure 5. Mohr's circle of stress for the matrix under thermally generated and applied stress components. The circle is centered at $\sigma = \sigma_Y/2$. Its radius is given by τ_{max}, as defined by Equation 11. θ is the angle between the planes of maximum shear stress and the whisker direction.

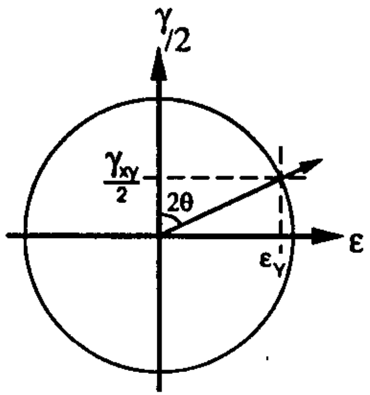

Figure 6. Mohr's circle of strain for the metal matrix under thermal cycling conditions. The diameter of the circle is set by $\Delta\gamma$ and the angle θ is determined by the construction in Figure 5. The intercepts ε_Y and γ_{XY} are the axial and shear strains as defined by the X-Y axes system.

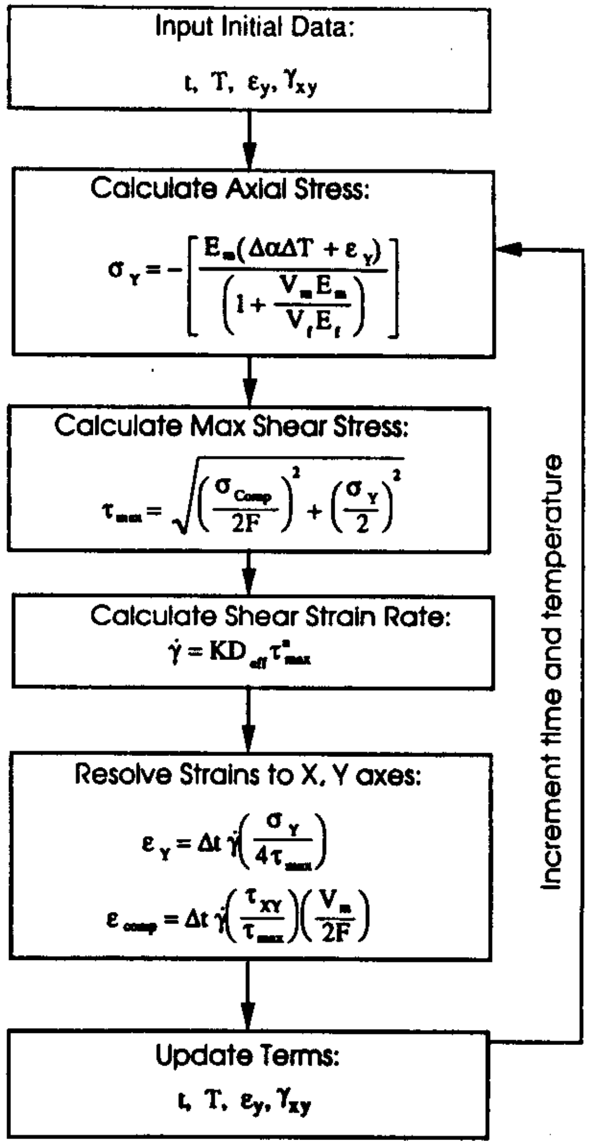

Figure 7. Flow chart of the computational steps involved with the simulation of creep of whisker reinforced composites, under thermal cycling conditions. The symbols represent values defined in the text.

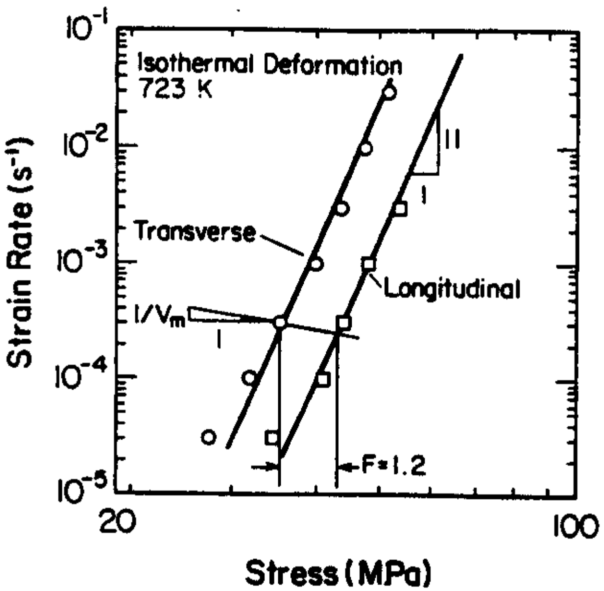

Figure 8. Isothermal stress v. strain-rate relationships for the longitudinal and transverse SiC reinforced Aluminum composites at 723 K. The geometric factor, F, is 1.2 in this case.

Figure 9a,b, c. Results of the simulation of the creep of a whisker reinforced composite under thermal cycling conditions at applied stresses σ_{comp} of 5 and 20 MPa. (a) shows the temperature cycle which was imposed. The axial stress in the matrix, σ_y as a function of time is shown in (b). Note that the magnitude of the stress drops in the late stages of heating cycles, and continues to rise during cooling. The plastic strains generated, ε_y (thermally induced) and ε_{comp} (composite elongation), are shown in (c). The slope of the ε_{comp} line with time gives the steady state, thermal cycling strain rate. The constants used in this and subsequent predictions are presented in Table 1.

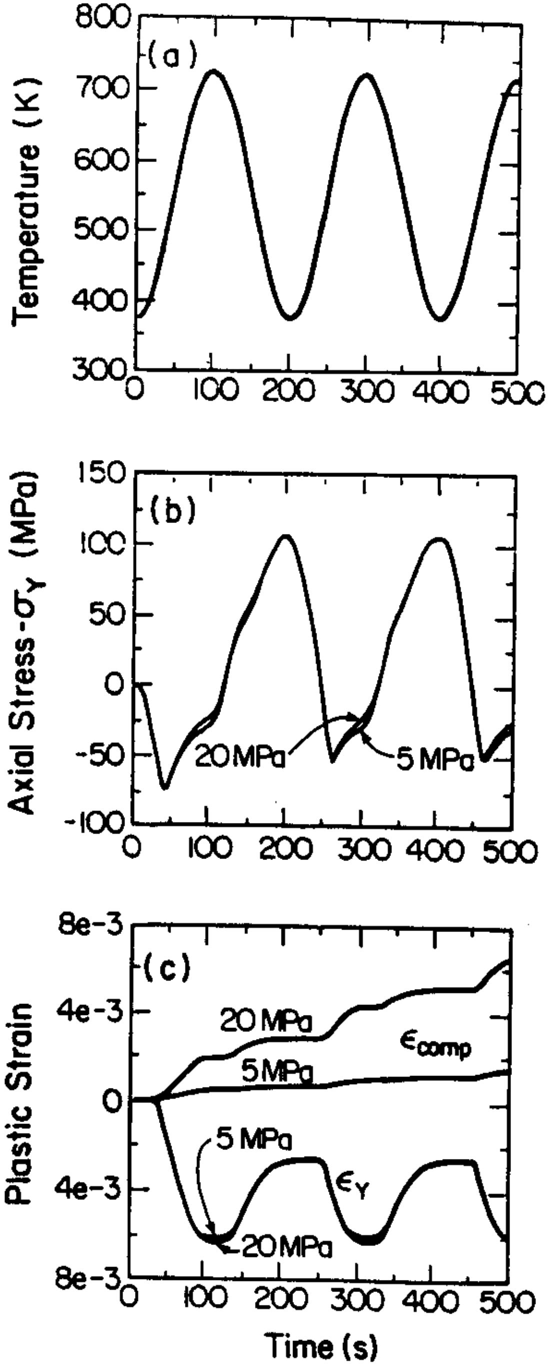

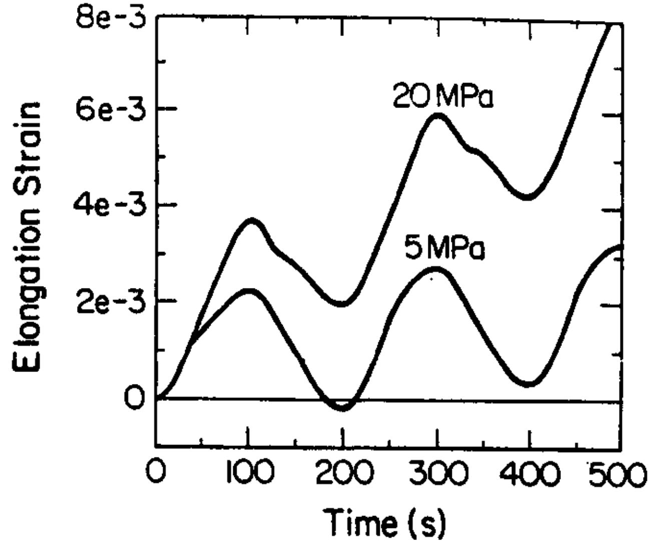

Figure 10a. During temperature cycling, thermal expansion and plastic elongation are concurrent. This demonstrates the relationship between the total elongation and time (Equation 20).

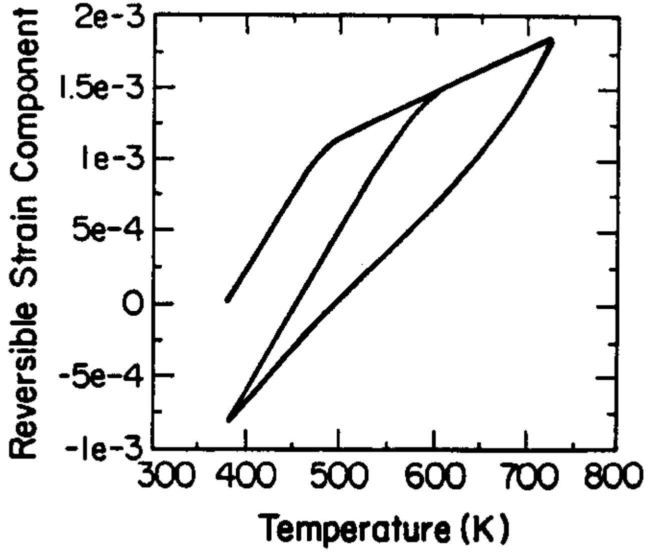

Figure 10b. Thermal strain of the composite ($\alpha_f(\Delta T) + E_f(\Delta\sigma^{...})$) as a function of temperature. Note the hysterisis in the this "reversible" strain component (i.e. total composite strain minus plastic elongation).

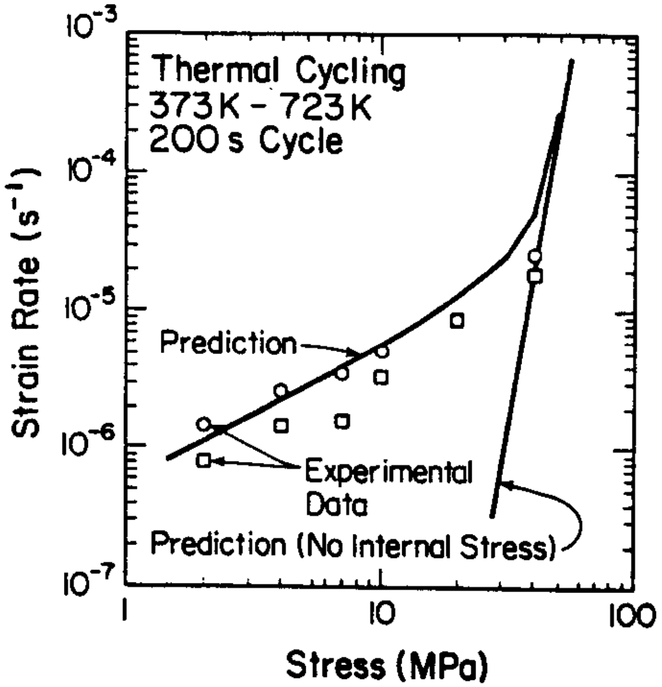

Figure 11. Thermal cycling strain-rate as a function of applied stress. The solid lines show the predicted behavior under thermal cycling, with and without a thermal expansion mismatch. The points represent experimental behavior, from two series of experiments (○ -single sample technique, □ -multiple sample technique). Both the simulations and experiments were run under thermal cycling conditions of 373 K to 723 K, in 200 second cycles.

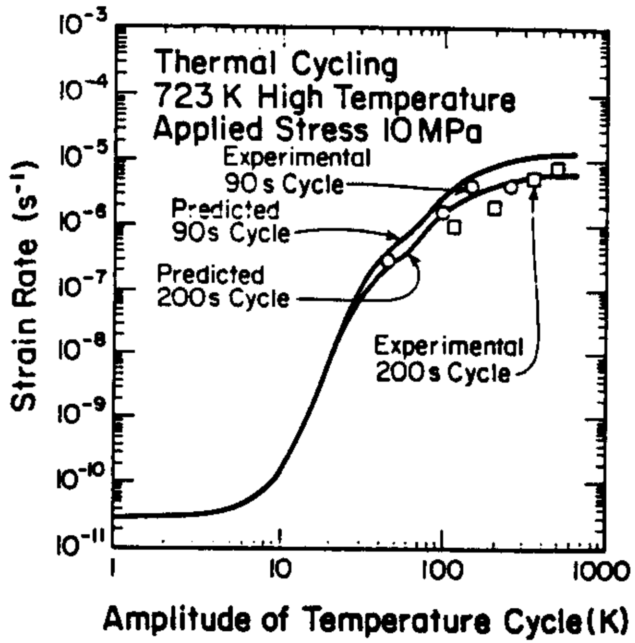

Figure 12. Comparison of experimental data to the model. In both the prediction and the experiments, the applied stress was 10 MPa and thermal cycles maintained a high temperature of 723 K, and variable amplitude. Two thermal cycling periods (90 seconds and 200 seconds) were used.

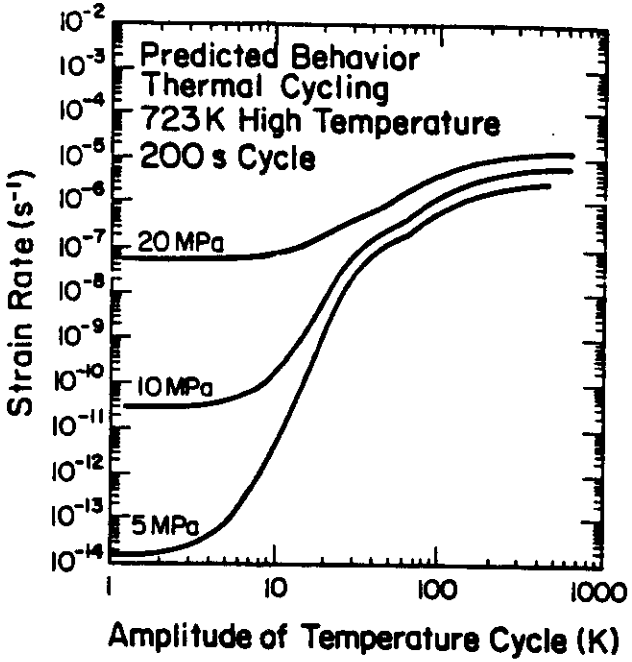

Figure 13. Effect of thermal cycle amplitude on steady state thermal cycling creep rate. These predictions were generated by imposing thermal cycles of a 200 second period which had a high temperature of 723 K and variable amplitude. Stresses of 5, 10 and 15 MPa were imposed.